Neural Computing and Applications (2022) 34:11123–11140
https://doi.org/10.1007/s00521-022-07032-8

ORIGINAL ARTICLE

Adaptive decentralized prescribed performance control for a class of large-scale nonlinear systems subject to nonsymmetric input saturations

Shan-Liang Zhu[1] · Yu-Qun Han[1]

Received: 3 August 2021 / Accepted: 30 January 2022 / Published online: 26 February 2022

Abstract
This paper investigates an adaptive decentralized predefined performance control problem for a class of large-scale nonlinear systems with nonsymmetric input saturation by using multi-dimensional taylor network (MTN) approach. Firstly, the input saturation model is approximated by a smooth function with a bounded approximation error and unknown nonlinear functions are estimated by MTNs. Secondly, a decentralized tracking control algorithm is established by integrating the idea of prescribed performance control into backstepping recursive technique. Thirdly, by using the designed MTN-based adaptive decentralized controller, all the closed-loop signals are bounded and all the tracking errors satisfy the predefined transient and steady-state performance, respectively. Finally, the presented control method is effective by introducing three examples, and the simulation results verify that the correctness and reasonableness of the proposed control algorithm.

Keywords Prescribed performance · Input saturation · Large-scale nonlinear systems · Adaptive control · Multi-dimensional Taylor network

1 Introduction

Generally speaking, large-scale systems can be regarded as a combination of some lower-order subsystems, which is widely used especially in power systems and economic systems. Because of the features of the information exchange among subsystems and the complexity of system, make it even trickier to controller design and stability analysis. Therefore, more and more attention has been transferred to the study of large-scale nonlinear systems in recent years [1–3]. In view of the decentralized control method is only depending on local information, the decentralized control technique has become an important control method to deal with the problems of control strategy for large-scale nonlinear systems, and many achievements have been achieved [4–6]. However, the aforementioned control approaches are suitable for the nonlinear systems satisfying the matching conditions or the unknown nonlinear functions can be linearly parameterized.

To attack these problems, many approximation-based intelligent control methods, for instance, fuzzy control, neural network (NN) control, and multi-dimensional Taylor network (MTN) control, have been extended to tackle the control problem of different types of nonlinear systems, such as general nonlinear systems [7–9], stochastic nonlinear systems [10–12], large-scale stochastic nonlinear systems [13–15], stochastic switched nonlinear systems [16, 17], and multi-input multi-output (MIMO) nonlinear systems [18]. Especially, by combining approximation-based control approach and adaptive decentralized control approach, many adaptive decentralized control algorithms have been put forward. For instance, for a class of large-scale nonlinear systems with actuator faults, authors in [19] presented a decentralized fault-tolerant control strategy. Authors in [20] developed a novel decentralized fuzzy-

✉ Yu-Qun Han
yuqunhan@qust.edu.cn

Shan-Liang Zhu
zhushanliang@qust.edu.cn

[1] School of Mathematics and Physics, Qingdao University of Science and Technology, Qingdao 266061, China

based adaptive optimal control approach for a class of large-scale nonlinear systems. For a class of switched large-scale nonlinear systems, authors in [21] proposed a switched observer-based decentralized adaptive fuzzy output-feedback control algorithm. For high-order stochastic nonlinear time-delay systems, authors in [22] developed a new decentralized NN-based adaptive control strategy. Authors in [23] addressed the problem of a class of strongly interconnected nonlinear systems and proposed an observer-NN-based adaptive decentralized control strategy. Authors in [24] investigated the event-triggered adaptive decentralized fuzzy control strategy for a class of large-scale nonlinear systems in a nonstrict-feedback structure. Although many approximation-based control adaptive decentralized control methods have been proposed for large-scale nonlinear systems, these control schemes can be not directly used to solve the problem of large-scale nonlinear systems subject to prescribed performance and nonsymmetric input saturation.

Actuators saturation is widely existence in practical engineering systems, however, it will deteriorate the control performance of systems or even destroy the stability of nonlinear systems. Therefore, research on the control strategy for nonlinear systems with input saturation has important theoretical and practical significance, and many significant results have been developed for different systems, such as uncertain nonaffine nonlinear systems [25], uncertain nonlinear switched systems with unmodeled dynamics [26], stochastic nonlinear systems [27, 28], MIMO nonlinear systems [29, 30], multi-agent uncertain systems [31]. On the other hand, owing to the fact that not only the stability of the system but also the features of steady-state operation and transient should be guaranteed in many industrial processes, prescribed performance control has been concerned by more and more researchers [32, 33]. To go a step further, as an important part of cybernetics, the problem of prescribed performance control of control systems subject to input saturation constraint has also been an active topic [34, 35]. Unfortunately, there tends to be a lack of development has been devoted to large-scale nonlinear systems subject to prescribed performance and nonsymmetric input saturation, and it is necessary to propose an approximation-based control method using MTN.

Based on the above observations, this paper pours attention into the tracking control problem for a class of large-scale nonlinear systems in the presence of input saturation and prescribed performance. A continuous smooth function is exploited to approximate the input saturation model; MTNs are introduced to estimate nonlinear functions. Then, an adaptive decentralized control algorithm is proposed via backstepping control technique and prescribed performance control. Compared with the existing results, the main innovations of this paper include:

1. For the first time, the MTN-based adaptive decentralized tracking control approach is generalised to a class of large-scale nonlinear systems, where the problems of prescribed performance and input saturation are considered simultaneously. Meanwhile, an adaptive decentralized control strategy is proposed that can ensure that all the tracking errors are constrained within the predefined values.
2. Unlike the existing results [27, 29, 36–38] only focused on the problem of input constrained, and the work of [39–42] only considered the problem of prescribed performance control, we simultaneously consider input saturations and prescribed performance control. Although similar control problems are also studied in [43–46], they all considered the single-input single-output (SISO) nonlinear systems. In addition, compared with the the problems of input saturation studied in [27, 37], the investigated nonsymmetric input saturations in this article are more general.
3. By introducing a smooth function to approximate the saturation nonlinearity model, and integrating the idea of prescribed performance control into backstepping technique, a new MTN-based decentralized adaptive control approach is developed, which be able to overcome the nonsymmetric input saturation problem of large-scale nonlinear systems.
4. In the process of controller design, although the traditional NNs or fuzzy logic systems (FLSs) can also be used to approximate the unknown nonlinear functions, MTNs can get the same effect at the cost of low computational complexity. Therefore, the MTN-based control strategy proposed in this paper is more suitable for practical applications.

2 Problem formulations and preliminaries

2.1 System description

In this paper, we consider the following large-scale nonlinear system consisting of N subsystems

$$\begin{cases} \dot{x}_{i,1} = x_{i,2} + f_{i,1}(\boldsymbol{x}_{i,1}) + h_{i,1}(\boldsymbol{y}) \\ \dot{x}_{i,j} = x_{i,j+1} + f_{i,j}(\boldsymbol{x}_{i,j}) + h_{i,j}(\boldsymbol{y}) \\ \quad j = 2, \ldots, n_{i-1} \\ \dot{x}_{i,n_i} = u_i + f_{i,n_i}(\boldsymbol{x}_{i,n_i}) + h_{i,n_i}(\boldsymbol{y}) \\ \quad y_i = x_{i,1} \end{cases} \tag{1}$$

where $i = 1, \ldots, N$. $y_i \in R$ denotes the scalar output of ith subsystem and $\boldsymbol{y} = [y_1, \ldots, y_N]^{\mathrm{T}} \in R^N$; $\boldsymbol{x}_{i,n_i} = [x_{i,1}, \ldots, x_{i,n_i}]^{\mathrm{T}} \in R^{n_i}$ denotes the state vector of ith subsystem and $\boldsymbol{x}_{i,j} = [x_{i,1}, \ldots, x_{i,j}]^{\mathrm{T}} \in R^j$. $f_{i,j}(\cdot) : R^j \rightarrow R$ denotes the unknown smooth function with $f_{i,j}(\boldsymbol{0}) = 0$. $h_{i,j}(\cdot) : R^N \rightarrow R$ denotes the interconnection between each subsystems and satisfies $h_{i,j}(0) = 0$. In particular, $u_i \in R$ denotes the scalar input of ith subsystem with nonsymmetric saturation nonlinearity and its mathematical model can be described as follows

$$u_i = S_i(v_i) = \begin{cases} u_{M,i}, v_i > u_{M,i} \\ v_i, -u_{m,i} \leq v_i \leq u_{M,i} \\ -u_{m,i}, v_i < -u_{m,i} \end{cases} \tag{2}$$

where $u_{M,i} > 0$ and $u_{m,i} > 0$ are the maximum bound and the minimum bound of the u_i, respectively. $v_i(t)$ are the inputs of the saturated model, which will be designed later.

Remark 1 One thing that should be pointed out is that system (1) can generalize many physical systems such as inverted pendulums [51, 52]. However, there are still several issues, such as time-varying delays [1, 2], input constraints [18], and actuator faults [19], that cannot ascribe to systems (1).

For the given desired trajectories $y_{d,i}, i = 1, \ldots, N$, a decentralized control strategy will be designed in this paper for system (1) to achieve the following control objectives, including

(i) The system output y_i can asymptotic track $y_{d,i}, i = 1, \ldots, N$, respectively. Furthermore, all the signals in the closed-loop system are bounded.
(ii) For every $i \in \{1, 2, \ldots, N\}$, the tracking error $e_i = y_i - y_{d,i}$ always satisfies the given predefined transient and steady-state performance.

2.2 Preliminaries and relative definition

Firstly, in view of the input saturation model (2) has two sharp corners, the control input $u_i (i = 1, 2, \ldots, N)$ cannot be directly constructed via backstepping technique. Therefore, in this paper, by using methods of [47], for each of $i = 1, \ldots, N$, $S_i(v_i)$ can be approximated by a smooth function $\hat{S}_i(v_i)$ with a bounded approximation error $B_i(v_i)$. Specifically,

$$S_i(v_i) = \hat{S}_i(v_i) + B_i(v_i) \tag{3}$$

where $\hat{S}_i(v_i) = \begin{cases} u_{M,i} \tanh\left(v_i/u_{M,i}\right), v_i \geq 0 \\ u_{m,i} \tanh\left(v_i/u_{m,i}\right), v_i < 0 \end{cases}$ and $|B_i(v_i)| \leq b_i$ with b_i is a constant.

In addition, for the smooth function $\hat{S}_i(v_i)$, according to the mean-value theorem, there exists a constant ϑ_i, such that $\hat{S}_i(v_i) = \hat{S}_i(v_{i,0}) + \hat{S}_{v_{i,\vartheta_i}} \cdot (v_i - v_{i,0})$, where $\hat{S}_{v_{i,\vartheta_i}} = (\partial S_i / \partial v_i)|_{v_i = v_{i,\vartheta_i}}$ and $v_{i,\vartheta_i} = \vartheta_i v_i + (1 - \vartheta_i) v_{i,0}$. Without loss of generality, choosing $v_{i,0} = 0$, we have

$$\hat{S}_i(v_i) = \hat{S}_{v_{i,\vartheta_i}} \cdot v_i \tag{4}$$

Secondly, in order to achieve the control objective (ii), a bounded prescribed performance function $\rho_i(t)$ can be designed for the tracking error $e_i(t) = y_i(t) - y_{d,i}(t)$, such that $|e_i(t)| < \rho_i(t)$, for $t \geq 0$. According to [40], in this paper, the $\rho_i(t)$ is formulated as

$$\rho_i(t) = (\rho_{i,0} - \rho_{i,\infty}) e^{-\ell_i t} + \rho_{i,\infty} \tag{5}$$

where $\rho_{i,0} > 0$, $\rho_{i,\infty} > 0$ and $\ell_i > 0$ are positive constants.

Thirdly, in the design of the controller design process, MTN will be employed to approximate the continuous function on a compact set. Then, the following approximation property of MTN is given.

Lemma 1 [15, 36, 48]: For a continuous function $f(\boldsymbol{\chi}) : R^n \rightarrow R$ defined on a compact set $\Omega \subset R^n$, there exists a MTN with form $\boldsymbol{\theta}^{\mathrm{T}} P_{m_n}(\boldsymbol{\chi})$, which has n inputs, and the highest power of middle layer is m, for $\forall \varepsilon > 0$, we have

$$f(\boldsymbol{\chi}) = \boldsymbol{\theta}^{\mathrm{T}} P_{m_n}(\boldsymbol{\chi}) + \delta(\boldsymbol{\chi}), \ |\delta(\boldsymbol{\chi})| \leq \varepsilon \tag{6}$$

where $\boldsymbol{\chi} = [\chi_1, \ldots, \chi_n]^{\mathrm{T}} \in R^m$, $\boldsymbol{\theta} = [\theta_1, \ldots, \theta_l]^{\mathrm{T}} \in R^l$ is the weight vector, $P_{m_n}(\boldsymbol{\chi}) = [\chi_1, \ldots, \chi_n, \chi_1^2, \chi_1 \chi_2, \ldots, \chi_n^2, \ldots, \chi_1^m, \ldots, \chi_n^m]^{\mathrm{T}} \in R^l$, $\delta(\boldsymbol{\chi})$ denotes the approximation error.

Remark 2 It is of interest to note that more information about MTN can be found in [14, 15].

Remark 3 It is worth noting that the fuzzy logic systems (FLSs) and NNs are also useful to approximate the unknown nonlinear functions in the systems, and many approximation-based adaptive fuzzy or NN control schemes have been put forward for different systems [53–55]. However, a few of them focused on prescribed control and input saturations for large-scale nonlinear systems simultaneity.

Finally, the following assumptions are given for the convenience of controller design.

Assumption 1 The reference signals $y_{d,i}$ and $y_{d,i}^{(k)}$ are continuous and bounded, where $y_{d,i}^{(k)}$ denotes the kth order time derivative of $y_{d,i}$, for $k = 1, \ldots, n_i$.

Assumption 2 For the functions $h_{i,j}(\boldsymbol{y})$, there exist analytic functions $h_{i,j,l}(y_l)$, such that

$$\left|h_{i,j}(\boldsymbol{y})\right|^2 \le \sum_{l=1}^{N} h_{i,j,l}^2(y_l) \tag{7}$$

with $h_{i,i,l}(0)=0$. Further more, according to mean value theorem, there exists function $\bar{h}_{i,j,l}(y_l)$, such that the following result holds

$$h_{i,j,l}(y_l) = y_l \bar{h}_{i,j,l}(y_l) \tag{8}$$

Remark 4 For the tracking control problem of nonlinear systems, Assumption 1 is reasonable. Meanwhile, for the adaptive decentralized controller design for large-scale nonlinear systems, Assumption 2 is a very common assumption adopted widely [49, 50].

Assumption 3 For each $i=1,\ldots,N$, there exists a positive constant s_i, such that

$$0 < s_i \le \hat{S}_{v_{i,\vartheta_i}} \le 1 \tag{9}$$

Assumption 4 All the states of the system are measurable. This means that all the states of system (1) can be used for controller design.

Remark 5 Assumption 3 is reasonable from the practical point of view, because the actual input of the control system cannot be infinite. In addition, Assumption 3 is commonly used for an adaptive control strategy for nonlinear systems with input saturation [28, 45, 47].

3 Controller design and stability analysis

First of all, the following form of coordinate transformation is employed in this paper.

$$\begin{cases} z_{i,1} = x_{i,1} - y_{d,i} \\ z_{i,j} = x_{i,j} - \alpha_{i,j-1} \end{cases} \tag{10}$$

where $i=1,\ldots,N, j=2,\ldots,n_i$, $\alpha_{i,j-1}$ represent the virtual control signals will be designed later via backstepping technique.

3.1 Decentralized adaptive controller design

Step i, 1: Choose the Lyapunov function as follows

$$V_{i,1} = \frac{1}{4}\xi_i^2 + \frac{1}{2}\tilde{\boldsymbol{\theta}}_{i,1}^{\mathrm{T}} \Gamma_{i,1}^{-1} \tilde{\boldsymbol{\theta}}_{i,1} \tag{11}$$

where $\xi_i = \frac{e_i^2}{\rho_i^2 - e_i^2}$, and $\tilde{\boldsymbol{\theta}}_{i,1} = \boldsymbol{\theta}_{i,1} - \hat{\boldsymbol{\theta}}_{i,1}$ denotes the parameter error vector, with $\boldsymbol{\theta}_{i,1}$ denotes the weight vector of MTN, which will be given later, $\hat{\boldsymbol{\theta}}_{i,1}$ denotes the estimation of $\boldsymbol{\theta}_{i,1}$. $\Gamma_{i,1} > 0$ denotes any positive definite matrix.

Then, calculating the time derivative of $V_{i,1}$, we have

$$\begin{aligned} \dot{V}_{i,1} &= \xi_i\left(\rho_{i,e}x_{i,2} + \rho_{i,e}f_{i,1} - \rho_{i,e}\dot{y}_{d,i} - \rho_{i,e}e_i\frac{\dot{\rho}_i}{\rho_i}\right) \\ &\quad + \xi_i\rho_{i,e}h_{i,1}(\boldsymbol{y}) - \tilde{\boldsymbol{\theta}}_{i,1}^{\mathrm{T}}\Gamma_{i,1}^{-1}\dot{\hat{\boldsymbol{\theta}}}_{i,1} \end{aligned} \tag{12}$$

where $\rho_{i,e} = \frac{e_i\rho_i^2}{\left(\rho_i^2 - e_i^2\right)^2}$.

According to Assumption 2, the following inequality can be obtained

$$\begin{aligned} \rho_{i,e}\xi_i h_{i,1}(\boldsymbol{y}) &\le \frac{1}{2}\rho_{i,e}^2\xi_i^2 + \frac{1}{2}h_{i,1}^2(\boldsymbol{y}) \\ &\le \frac{1}{2}\rho_{i,e}^2\xi_i^2 + \frac{1}{2}\sum_{l=1}^{N} y_l^2\bar{h}_{i,1,l}^2(y_l) \end{aligned} \tag{13}$$

Next, substituting (13) into (12), the following inequality can be obtained

$$\begin{aligned} \dot{V}_{i,1} &\le \xi_i\left(\rho_{i,e}x_{i,2} + \rho_{i,e}f_{i,1} - \rho_{i,e}\dot{y}_{d,i} - \rho_{i,e}e_i\frac{\dot{\rho}_i}{\rho_i}\right) \\ &\quad + \frac{1}{2}\rho_{i,e}^2\xi_i^2 + \frac{1}{2}\sum_{l=1}^{N} y_l^2\bar{h}_{i,1,l}^2(y_l) - \tilde{\boldsymbol{\theta}}_{i,1}^{\mathrm{T}}\Gamma_{i,1}^{-1}\dot{\hat{\boldsymbol{\theta}}}_{i,1} \\ &= \xi_i\left(\rho_{i,e}x_{i,2} + \bar{f}_{i,1}\right) - \frac{1}{2}\xi_i^2 - \omega_i\left(\xi_i^2\right)\xi_i^2 \\ &\quad + \frac{1}{2}\sum_{l=1}^{N} y_l^2\bar{h}_{i,1,l}^2(y_l) - \tilde{\boldsymbol{\theta}}_{i,1}^{\mathrm{T}}\Gamma_{i,1}^{-1}\dot{\hat{\boldsymbol{\theta}}}_{i,1} \end{aligned} \tag{14}$$

where $\bar{f}_{i,1} = \rho_{i,e}f_{i,1} - \rho_{i,e}\dot{y}_{d,i} - \rho_{i,e}e_i\frac{\dot{\rho}_i}{\rho_i} + \frac{1}{2}\xi_i\rho_{i,e}^2 + \omega_i\left(\xi_i^2\right)\xi_i + \frac{1}{2}\xi_i$.

Remark 6 $\omega_i(\cdot)$ is a positive definite auxiliary function, and its value is not necessary to be known since it not used for controller design.

Obviously, the unknown function $\bar{f}_{i,1}$ can not be directly used for virtual controller design. Therefore, by virtue of Lemma 1, $\bar{f}_{i,1}$ can be approximated by a MTN. Specifically, for any given control accuracy $\varepsilon_{i,1} > 0$, there exists a MTN $\boldsymbol{\theta}_{i,1}^{\mathrm{T}}P_{m_{i,1}}(\boldsymbol{\xi}_i)$ satisfies

$$\bar{f}_{i,1} = \boldsymbol{\theta}_{i,1}^{\mathrm{T}}P_{m_{i,1}}(\xi_i) + \delta_{i,1}(\xi_i) \tag{15}$$

where $\delta_{i,1}(\xi_i)$ denotes the approximation error and satisfies $\left|\delta_{i,1}(\xi_i)\right| \le \varepsilon_{i,1}$.

In view of $x_{i,2} = z_{i,2} + \alpha_{i,1}$, and substituting (15) into (14), we have

$$\dot{V}_{i,1} \le \xi_i\left(\rho_{i,e}x_{i,2} + \boldsymbol{\theta}_{i,1}^{\mathrm{T}}P_{m_{i,1}}\right) - \frac{1}{2}\xi_i^2 + \xi_i\delta_{i,1} - \omega_i\left(\xi_i^2\right)\xi_i^2 + \frac{1}{2}\sum_{l=1}^{N} y_l^2\bar{h}_{i,1,l}^2(y_l) - \tilde{\boldsymbol{\theta}}_{i,1}^{\mathrm{T}}\Gamma_{i,1}^{-1}\dot{\hat{\boldsymbol{\theta}}}_{i,1}$$
$$\le \xi_i\left(\rho_{i,e}z_{i,2} + \rho_{i,e}\alpha_{i,1} + \boldsymbol{\theta}_{i,1}^{\mathrm{T}}P_{m_{i,1}}\right) + \frac{1}{2}\varepsilon_{i,1}^2 - \omega_i\left(\xi_i^2\right)\xi_i^2 + \frac{1}{2}\sum_{l=1}^{N} y_l^2\bar{h}_{i,1,l}^2(y_l) - \tilde{\boldsymbol{\theta}}_{i,1}^{\mathrm{T}}\Gamma_{i,1}^{-1}\dot{\hat{\boldsymbol{\theta}}}_{i,1} \tag{16}$$

According to inequality (16), the virtual control signal $\alpha_{i,1}$ can be designed as follows

$$\alpha_{i,1} = -\frac{1}{\rho_{i,e}}\left(\gamma_{i,1}\xi_i + \hat{\boldsymbol{\theta}}_{i,1}^{\mathrm{T}}P_{m_{i,1}}\right) \tag{17}$$

where $\gamma_{i,1} > 0$.

Substituting (17) into (16), we have

$$\dot{V}_{i,1} \le -\gamma_{i,1}\xi_i^2 + \xi_i\rho_{i,e}z_{i,2} - \omega_i(\xi_i)\xi_i^2 + \frac{1}{2}\sum_{l=1}^{N} y_l^2\bar{h}_{i,1,l}^2(y_l) + \frac{1}{2}\varepsilon_{i,1}^2 + \tilde{\boldsymbol{\theta}}_{i,1}^{\mathrm{T}}\left(\xi_iP_{m_{i,1}} - \Gamma_{i,1}^{-1}\dot{\hat{\boldsymbol{\theta}}}_{i,1}\right) \tag{18}$$

Remark 7 In this step, a new variable ξ_i incorporating the predefined performance function is introduced, then the issue of the predefined control performance is solved by employing the Lyapunov function (11), thus achieving the tracking error e_i satisfies the given prescribed performance.

Step i, 2: Choosing the Lyapunov function as follows

$$V_{i,2} = V_{i,1} + \frac{1}{2}z_{i,2}^2 + \frac{1}{2}\tilde{\boldsymbol{\theta}}_{i,2}^{\mathrm{T}}\Gamma_{i,2}^{-1}\tilde{\boldsymbol{\theta}}_{i,2} \tag{19}$$

where $\tilde{\boldsymbol{\theta}}_{i,2} = \boldsymbol{\theta}_{i,2} - \hat{\boldsymbol{\theta}}_{i,2}$ is the parameter error vector, with $\boldsymbol{\theta}_{i,2}$ denotes the weight vector of MTN, which will be given later, $\hat{\boldsymbol{\theta}}_{i,2}$ denotes the estimation of $\boldsymbol{\theta}_{i,2}$. $\Gamma_{i,2}$ is any positive definite matrix.

Then, calculating the time derivative of $V_{i,2}$, we have

$$\dot{V}_{i,2} = \dot{V}_{i,1} + z_{i,2}\left(x_{i,3} + f_{i,2} + h_{i,2}(\boldsymbol{y}) - \dot{\alpha}_{i,1}\right) - \tilde{\boldsymbol{\theta}}_{i,2}^{\mathrm{T}}\Gamma_{i,2}^{-1}\dot{\hat{\boldsymbol{\theta}}}_{i,2} \tag{20}$$

According to Assumption 2, the following inequality can be obtained

$$z_{i,2}h_{i,2}(\boldsymbol{y}) \le \frac{1}{2}z_{i,2}^2 + \frac{1}{2}h_{i,2}^2(\boldsymbol{y}) \le \frac{1}{2}z_{i,2}^2 + \frac{1}{2}\sum_{l=1}^{N} y_l^2\bar{h}_{i,2,l}^2(y_l) \tag{21}$$

Substituting (21) into (20), the following inequality can be obtained

$$\dot{V}_{i,2} \le \dot{V}_{i,1} + z_{i,2}\left(x_{i,3} + f_{i,2} + \xi_i\rho_{i,e} - \dot{\alpha}_{i,1}\right) - \xi_i\rho_{i,e}z_{i,2} + \frac{1}{2}z_{i,2}^2 + \frac{1}{2}\sum_{l=1}^{N} y_l^2\bar{h}_{i,2,l}^2(y_l) - \tilde{\boldsymbol{\theta}}_{i,2}^{\mathrm{T}}\Gamma_{i,2}^{-1}\dot{\hat{\boldsymbol{\theta}}}_{i,2}$$
$$= \dot{V}_{i,1} + z_{i,2}\left(x_{i,3} + \bar{f}_{i,2}\right) - \xi_i\rho_{i,e}z_{i,2} - z_{i,2}^2 + \frac{1}{2}\sum_{l=1}^{N} y_l^2\bar{h}_{i,2,l}^2(y_l) - \tilde{\boldsymbol{\theta}}_{i,2}^{\mathrm{T}}\Gamma_{i,2}^{-1}\dot{\hat{\boldsymbol{\theta}}}_{i,2} \tag{22}$$

where $\bar{f}_{i,2} = f_{i,2} + \xi_i\rho_{i,e} + \frac{3}{2}z_{i,2} - \dot{\alpha}_{i,1}$.

Similarly, the unknown function $\bar{f}_{i,2}$ can not be directly used for virtual controller design. Therefore, by virtue of Lemma 1, $\bar{f}_{i,2}$ can be approximated by a MTN. Specifically, for any given control accuracy $\varepsilon_{i,2} > 0$, there exists a MTN $\boldsymbol{\theta}_{i,2}^{\mathrm{T}}P_{m_{i,2}}\left(Z_{i,2}\right)$ satisfies

$$\bar{f}_{i,2} = \boldsymbol{\theta}_{i,2}^{\mathrm{T}}P_{m_{i,2}}\left(Z_{i,2}\right) + \delta_{i,2}\left(Z_{i,2}\right) \tag{23}$$

where $\delta_{i,2}\left(Z_{i,2}\right)$ denotes the approximation error and satisfies $\left|\delta_{i,2}\left(Z_{i,2}\right)\right| \le \varepsilon_{i,2}$.

In view of $x_{i,3} = z_{i,3} + \alpha_{i,2}$ and substituting (23) into (22), we have

$$\dot{V}_{i,2} \le \dot{V}_{i,1} + z_{i,2}\left(z_{i,3} + \alpha_{i,2} + \boldsymbol{\theta}_{i,2}^{\mathrm{T}}P_{m_{i,2}}\right) - \frac{1}{2}z_{i,2}^2 + \frac{1}{2}\varepsilon_{i,2}^2 - \xi_i\rho_{i,e}z_{i,2} + \frac{1}{2}\sum_{l=1}^{N} y_l^2\bar{h}_{i,2,l}^2(y_l) - \tilde{\boldsymbol{\theta}}_{i,2}^{\mathrm{T}}\Gamma_{i,2}^{-1}\dot{\hat{\boldsymbol{\theta}}}_{i,2} \tag{24}$$

According to inequality (24), the virtual control signal $\alpha_{i,2}$ can be designed as follows

$$\alpha_{i,2} = -\gamma_{i,2}z_{i,2} - \hat{\boldsymbol{\theta}}_{i,2}^{\mathrm{T}}P_{m_{i,2}} \tag{25}$$

where $\gamma_{i,2} > 0$.

Substituting (18) and (25) into (24), we have

$$\dot{V}_{i,2} \le -\gamma_{i,1}\xi_i^2 - \gamma_{i,2}z_{i,2}^2 + z_{i,2}z_{i,3} - \frac{1}{2}z_{i,2}^2 - \omega_i\left(\xi_i^2\right)\xi_i^2 + \frac{1}{2}\sum_{j=1}^{2}\sum_{l=1}^{N} y_l^2 \bar{h}_{i,j,l}^2(y_l) + \frac{1}{2}\sum_{j=1}^{2}\varepsilon_{i,j}^2 + \tilde{\boldsymbol{\theta}}_{i,1}^{\mathrm{T}}\left(\xi_i P_{m_{i,1}} - \Gamma_{i,1}^{-1}\dot{\hat{\boldsymbol{\theta}}}_{i,1}\right) + \tilde{\boldsymbol{\theta}}_{i,2}^{\mathrm{T}}\left(z_{i,2}P_{m_{i,2}} - \Gamma_{i,2}^{-1}\dot{\hat{\boldsymbol{\theta}}}_{i,2}\right) \tag{26}$$

In light of $z_{i,2}z_{i,3} \le \frac{1}{2}z_{i,2}^2 + \frac{1}{2}z_{i,3}^2$, (26) becomes

$$\dot{V}_{i,2} \le -\gamma_{i,1}\xi_i^2 - \gamma_{i,2}z_{i,2}^2 + \frac{1}{2}z_{i,3}^2 - \omega_i\left(\xi_i^2\right)\xi_i^2 + \frac{1}{2}\sum_{j=1}^{2}\sum_{l=1}^{N} y_l^2 \bar{h}_{i,j,l}^2(y_l) + \frac{1}{2}\sum_{j=1}^{2}\varepsilon_{i,j}^2 + \tilde{\boldsymbol{\theta}}_{i,1}^{\mathrm{T}}\left(\xi_i P_{m_{i,1}} - \Gamma_{i,1}^{-1}\dot{\hat{\boldsymbol{\theta}}}_{i,1}\right) + \tilde{\boldsymbol{\theta}}_{i,2}^{\mathrm{T}}\left(z_{i,2}P_{m_{i,2}} - \Gamma_{i,2}^{-1}\dot{\hat{\boldsymbol{\theta}}}_{i,2}\right) \tag{27}$$

Step i,k $(3 \le k \le n_{i-1})$: Choosing the Lyapunov function as follows

$$V_{i,k} = V_{i,k-1} + \frac{1}{2}z_{i,k}^2 + \frac{1}{2}\tilde{\boldsymbol{\theta}}_{i,k}^{\mathrm{T}}\Gamma_{i,k}^{-1}\tilde{\boldsymbol{\theta}}_{i,k} \tag{28}$$

where $\tilde{\boldsymbol{\theta}}_{i,k} = \boldsymbol{\theta}_{i,k} - \hat{\boldsymbol{\theta}}_{i,k}$ is the parameter error vector, with $\boldsymbol{\theta}_{i,k}$ denotes the weight vector of MTN, which will be given later, $\hat{\boldsymbol{\theta}}_{i,k}$ denotes the estimation of $\boldsymbol{\theta}_{i,k}$. $\Gamma_{i,k}$ is any positive definite matrix.

Then, calculating the time derivative of $V_{i,k}$, we have

$$\dot{V}_{i,k} = z_{i,k}\left(x_{i,k+1} + f_{i,k} + h_{i,k}(\mathbf{y}) - \dot{\alpha}_{i,k-1}\right) + \dot{V}_{i,k-1} - \tilde{\boldsymbol{\theta}}_{i,k}^{\mathrm{T}}\Gamma_{i,k}^{-1}\dot{\hat{\boldsymbol{\theta}}}_{i,k} \tag{29}$$

According to Assumption 2, the following inequality can be obtained

$$z_{i,k}h_{i,k}(\mathbf{y}) \le \frac{1}{2}z_{i,k}^2 + \frac{1}{2}h_{i,k}^2(\mathbf{y}) \le \frac{1}{2}z_{i,k}^2 + \frac{1}{2}\sum_{l=1}^{N} y_l^2 \bar{h}_{i,k,l}^2(y_l) \tag{30}$$

Substituting (30) into (29), the following inequality can be obtained

$$\dot{V}_{i,k} = \dot{V}_{i,k-1} + z_{i,k}\left(x_{i,k+1} + \bar{f}_{i,k}\right) - \frac{3}{2}z_{i,k}^2 + \frac{1}{2}\sum_{l=1}^{N} y_l^2 \bar{h}_{i,k,l}^2(y_l) - \tilde{\boldsymbol{\theta}}_{i,k}^{\mathrm{T}}\Gamma_{i,k}^{-1}\dot{\hat{\boldsymbol{\theta}}}_{i,k} \tag{31}$$

where $\bar{f}_{i,k} = f_{i,k} + 2z_{i,k} - \dot{\alpha}_{i,k-1}$.

Similarly, the unknown function $\bar{f}_{i,k}$ can not be directly used for virtual controller design. Therefore, by virtue of Lemma 1, $\bar{f}_{i,k}$ can be approximated by a MTN. Specifically, for any given control accuracy $\varepsilon_{i,k} > 0$, there exists a MTN $\boldsymbol{\theta}_{i,k}^{\mathrm{T}}P_{m_{i,k}}\left(Z_{i,k}\right)$ satisfies

$$\bar{f}_{i,k} = \boldsymbol{\theta}_{i,k}^{\mathrm{T}}P_{m_{i,k}}\left(Z_{i,k}\right) + \delta_{i,k}\left(Z_{i,k}\right) \tag{32}$$

where $\delta_{i,k}\left(Z_{i,k}\right)$ denotes the approximation error and satisfies $\left|\delta_{i,k}\left(Z_{i,k}\right)\right| \le \varepsilon_{i,k}$, for $\varepsilon_{i,k} > 0$.

Considering $x_{i,k+1} = z_{i,k+1} + \alpha_{i,k}$ and substituting (32) into (31), we have

$$\dot{V}_{i,k} \le \dot{V}_{i,k-1} + z_{i,k}\left(z_{i,k+1} + \alpha_{i,k} + \boldsymbol{\theta}_{i,k}^{\mathrm{T}}P_{m_{i,k}}\right) - z_{i,k}^2 + \frac{1}{2}\varepsilon_{i,k}^2 + \frac{1}{2}\sum_{l=1}^{N} y_l^2 \bar{h}_{i,k,l}^2(y_l) - \tilde{\boldsymbol{\theta}}_{i,k}^{\mathrm{T}}\Gamma_{i,k}^{-1}\dot{\hat{\boldsymbol{\theta}}}_{i,k} \tag{33}$$

According to inequality (33), the virtual control signal $\alpha_{i,k}$ can be designed as follows

$$\alpha_{i,k} = -\gamma_{i,k}z_{i,k} - \hat{\boldsymbol{\theta}}_{i,k}^{\mathrm{T}}P_{m_{i,k}} \tag{34}$$

where $\gamma_{i,k} > 0$.

In light of $z_{i,k}z_{i,k+1} \le \frac{1}{2}z_{i,k}^2 + \frac{1}{2}z_{i,k+1}^2$, based on recurrence method and substituting (34) into (33), we have

$$\dot{V}_{i,k} \le -\gamma_{i,1}\xi_i^2 - \sum_{j=2}^{k}\gamma_{i,j}z_{i,j}^2 - \omega_i\left(\xi_i^2\right)\xi_i^2 + \frac{1}{2}z_{i,k+1}^2 + \frac{1}{2}\sum_{j=1}^{k}\sum_{l=1}^{N} y_l^2 \bar{h}_{i,j,l}^2(y_l) + \frac{1}{2}\sum_{j=1}^{k}\varepsilon_{i,j}^2 + \tilde{\boldsymbol{\theta}}_{i,1}^{\mathrm{T}}\left(\xi_i P_{m_{i,1}} - \Gamma_{i,1}^{-1}\dot{\hat{\boldsymbol{\theta}}}_{i,1}\right) + \sum_{j=2}^{k}\tilde{\boldsymbol{\theta}}_{i,j}^{\mathrm{T}}\left(z_{i,j}P_{m_{i,j}} - \Gamma_{i,j}^{-1}\dot{\hat{\boldsymbol{\theta}}}_{i,j}\right) \tag{35}$$

Step i, n_i: Choosing the Lyapunov function as follows

$$V_{i,n_i} = V_{i,n_i-1} + \frac{1}{2}z_{i,n_i}^2 + \frac{1}{2}\tilde{\boldsymbol{\theta}}_{i,n_i}^{\mathrm{T}}\Gamma_{i,n_i}^{-1}\tilde{\boldsymbol{\theta}}_{i,n_i} \tag{36}$$

where $\tilde{\boldsymbol{\theta}}_{i,n_i} = \boldsymbol{\theta}_{i,n_i} - \hat{\boldsymbol{\theta}}_{i,n_i}$ is the parameter error vector, with $\boldsymbol{\theta}_{i,n_i}$ denotes the weight vector of MTN, which will be given later, $\hat{\boldsymbol{\theta}}_{i,n_i}$ denotes the estimation of $\boldsymbol{\theta}_{i,n_i}$. Γ_{i,n_i} is any positive definite matrix.

In view of (4), calculating the time derivative of V_{i,n_i}, we have

$$\dot{V}_{i,n_i} = z_{i,n_i}\left(\hat{S}_{v_{i,\vartheta_i}} \cdot v_i + B_i + f_{i,n_i} + h_{i,n_i}(\mathbf{y}) - \dot{\alpha}_{i,n_i-1}\right) + \dot{V}_{i,n_{i-1}} - \tilde{\boldsymbol{\theta}}_{i,n_i}^{\mathrm{T}}\Gamma_{i,n_i}^{-1}\dot{\hat{\boldsymbol{\theta}}}_{i,n_i} \tag{37}$$

According to Assumption 2, the following inequality can be obtained

$$z_{i,n_i}h_{i,n_i}(\boldsymbol{y}) \le \frac{1}{2}z_{i,n_i}^2 + \frac{1}{2}h_{i,n_i}^2(\boldsymbol{y}) \le \frac{1}{2}z_{i,n_i}^2 + \frac{1}{2}\sum_{l=1}^{N} y_l^2 \bar{h}_{i,n_i,l}^2(y_l) \tag{38}$$

$$z_{i,n_i}B_i \le \frac{1}{2}z_{i,n_i}^2 + \frac{1}{2}b_i^2 \tag{39}$$

Substituting (38) and (39) into (37), the following inequality can be obtained

$$\begin{aligned}\dot{V}_{i,n_i} &= \dot{V}_{i,n_{i-1}} + z_{i,n_i}\left(\hat{S}_{v_{i,\vartheta_i}} \cdot v_i + f_{i,n_i} - \dot{\alpha}_{i,n_i-1}\right) \\ &\quad + \frac{1}{2}z_{i,n_i}^2 + \frac{1}{2}\sum_{l=1}^{N} y_l^2 \bar{h}_{i,n_i,l}^2(y_l) - \tilde{\boldsymbol{\theta}}_{i,n_i}^{\mathrm{T}}\Gamma_{i,n_i}^{-1}\dot{\hat{\boldsymbol{\theta}}}_{i,n_i} + \frac{1}{2}z_{i,n_i}^2 + \frac{1}{2}b_i^2 \\ &\le \dot{V}_{i,n_{i-1}} + z_{i,n_i}\left(\hat{S}_{v_{i,\vartheta_i}} \cdot v_i + \bar{f}_{i,n_i}\right) - z_{i,n_i}^2 \\ &\quad \frac{1}{2}\sum_{l=1}^{N} y_l^2 \bar{h}_{i,n_i,l}^2(y_l) - \tilde{\boldsymbol{\theta}}_{i,n_i}^{\mathrm{T}}\Gamma_{i,n_i}^{-1}\dot{\hat{\boldsymbol{\theta}}}_{i,n_i} + \frac{1}{2}b_i^2\end{aligned} \tag{40}$$

where $\bar{f}_{i,n_i} = f_{i,n_i} + 2z_{i,n_i} - \dot{\alpha}_{i,n_i-1}$.

Similarly, the unknown function $\bar{f}_{i,n_i}$ can not be directly used for virtual controller design. Therefore, by virtue of Lemma 1, $\bar{f}_{i,n_i}$ can be approximated by a MTN. Specifically, for any given control accuracy $\varepsilon_{i,n_i} > 0$, there exists a MTN $\boldsymbol{\theta}_{i,n_i}^{\mathrm{T}}P_{m_{i,n_i}}(Z_{i,n_i})$ satisfies

$$\bar{f}_{i,n_i} = \boldsymbol{\theta}_{i,n_i}^{\mathrm{T}}P_{m_{i,n_i}}(Z_{i,n_i}) + \delta_{i,n_i}(Z_{i,n_i}) \tag{41}$$

where $\delta_{i,n_i}(Z_{i,n_i})$ denotes the approximation error and satisfies $|\delta_{i,n_i}(Z_{i,n_i})| \le \varepsilon_{i,n_i}$.

Substituting (41) into (40), we have

$$\begin{aligned}\dot{V}_{i,n_i} &\le \dot{V}_{i,n_{i-1}} + z_{i,n_i}\left(\hat{S}_{v_{i,\vartheta_i}} \cdot v_i + \boldsymbol{\theta}_{i,n_i}^{\mathrm{T}}P_{m_{i,n_i}}\right) - \frac{1}{2}z_{i,n_i}^2 \\ &\quad + \frac{1}{2}\varepsilon_{i,n_i}^2 + \frac{1}{2}\sum_{l=1}^{N} y_l^2 \bar{h}_{i,n_i,l}^2(y_l) - \tilde{\boldsymbol{\theta}}_{i,n_i}^{\mathrm{T}}\Gamma_{i,n_i}^{-1}\dot{\hat{\boldsymbol{\theta}}}_{i,n_i} + \frac{1}{2}b_i^2\end{aligned} \tag{42}$$

Then, design the actual control signal v_i as follows

$$v_i = -\frac{1}{s_i}\left(\gamma_{i,n_i}|z_{i,n_i}| + \left|\hat{\boldsymbol{\theta}}_{i,n_i}^{\mathrm{T}}P_{m_{i,n_i}}\right|\right)\mathrm{sgn}(z_{i,n_i}) \tag{43}$$

where $\gamma_{i,n_i} > 0$ and $\mathrm{sgn}(\cdot)$ denotes sign function.

Then, in light of $z_{i,n_i}\hat{S}_{v_{i,\vartheta_i}} \cdot v_i \le -\gamma_{i,n_i}z_{i,n_i}^2 - |z_{i,n_i}\hat{\boldsymbol{\theta}}_{i,n_i}^{\mathrm{T}}P_{m_{i,n_i}}|$, and substituting (35) with $k = n_i - 1$ and (43) into (42), we have

$$\begin{aligned}\dot{V}_{i,n_{i-1}} &\le -\gamma_{i,1}\xi_i^2 - \sum_{j=2}^{n_i}\gamma_{i,j}z_{i,j}^2 - \omega_i(\xi_i^2)\xi_i^2 \\ &\quad + \frac{1}{2}\sum_{j=1}^{n_i}\sum_{l=1}^{N} y_l^2 \bar{h}_{i,j,l}^2(y_l) + \frac{1}{2}\sum_{j=1}^{n_i}\varepsilon_{i,j}^2 + \frac{1}{2}b_i^2 \\ &\quad + \tilde{\boldsymbol{\theta}}_{i,1}^{\mathrm{T}}\left(\xi_i P_{m_{i,1}} - \Gamma_{i,1}^{-1}\dot{\hat{\boldsymbol{\theta}}}_{i,1}\right) \\ &\quad + \sum_{j=2}^{n_i}\tilde{\boldsymbol{\theta}}_{i,j}^{\mathrm{T}}\left(z_{i,j}P_{m_{i,j}} - \Gamma_{i,j}^{-1}\dot{\hat{\boldsymbol{\theta}}}_{i,j}\right)\end{aligned} \tag{44}$$

This completes the design of controller. Next, the main results of this paper are illustrated by the following theorem.

Then the design procedure of the above-proposed control scheme is shown in Fig. 1.

Remark 8 It is worth noting that this paper failed to consider the robustness of the control strategy. As shown in [56, 57], the robustness of the controller can be improved by adding a compensator.

3.2 Stability analysis of closed-loop system

Theorem 1 *Under Assumptions 1-4, consider the closed-loop system comprised of a large-scale nonlinear system (1) with input saturation (2), the actual control input (43), the virtual control signals (17), (25), (34), along with the parameter laws are described as*

$$\begin{aligned}\dot{\hat{\boldsymbol{\theta}}}_{i,1} &= \xi_i\Gamma_{i,1}P_{m_{i,1}} - \eta_{i,1}\Gamma_{i,1}\hat{\boldsymbol{\theta}}_{i,1} \\ \dot{\hat{\boldsymbol{\theta}}}_{i,j} &= z_{i,j}\Gamma_{i,j}P_{m_{i,j}} - \eta_{i,j}\Gamma_{i,j}\hat{\boldsymbol{\theta}}_{i,j}\end{aligned} \tag{45}$$

with $i \in \{1,\ldots,N\}$, $j \in \{2,\ldots,n_i\}$. Then

(1) The system output y_i tracks the desired trajectory $y_{d,i}$, for every $i = 1,\ldots,N$. In addition, all the closed-loop signals are bounded.

(2) All the tracking errors $e_i = y_i - y_{d,i}$ satisfy the predefined transient and steady-state performance.

Proof For the whole closed loop system, choosing the Lyapunov function as follows

$$V = \frac{1}{4}\sum_{i=1}^{N}\xi_i^2 + \frac{1}{2}\sum_{i=1}^{N}\sum_{j=2}^{n_i}z_{i,j}^2 + \frac{1}{2}\sum_{i=1}^{N}\sum_{j=1}^{n_i}\tilde{\boldsymbol{\theta}}_{i,j}^{\mathrm{T}}\Gamma_{i,j}^{-1}\tilde{\boldsymbol{\theta}}_{i,j} \tag{46}$$

Then, according to (44), the time derivative of V is calculated as follows

Fig. 1 The structure of MTN

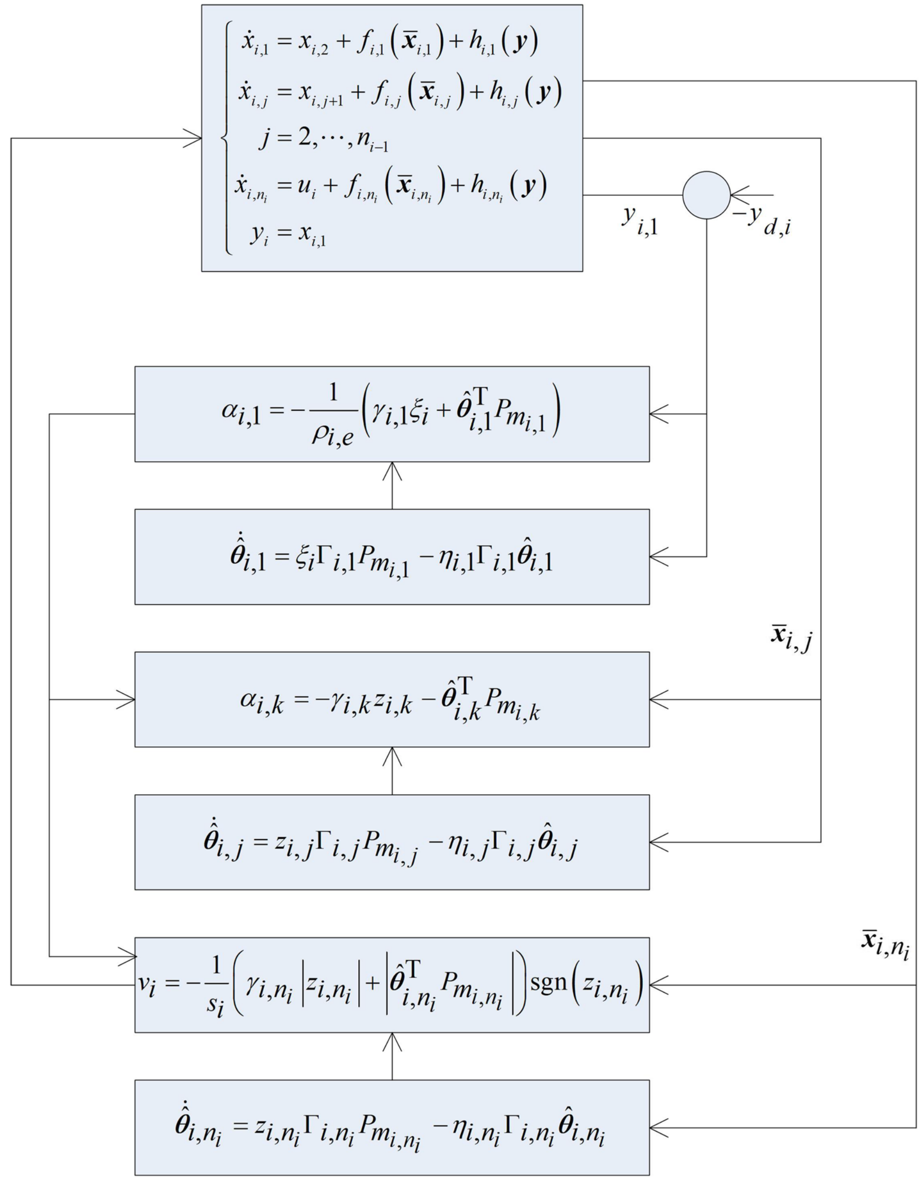

$$
\begin{aligned}
\dot{V} \le & -\sum_{i=1}^{N}\gamma_{i,1}\xi_i^2 - \sum_{i=1}^{N}\sum_{j=2}^{n_i}\gamma_{i,j}z_{i,j}^2 - \sum_{i=1}^{N}\omega_i\left(\xi_i^2\right)\xi_i^2 \\
& + \frac{1}{2}\sum_{i=1}^{N}\sum_{j=1}^{n_i}\sum_{l=1}^{N} y_l^2 \bar{h}_{i,j,l}^2(y_l) + \frac{1}{2}\sum_{i=1}^{N}\sum_{j=1}^{n_i}\varepsilon_{i,j}^2 + \frac{1}{2}b_i^2 \\
& + \sum_{i=1}^{N}\tilde{\boldsymbol{\theta}}_{i,1}^{\mathrm{T}}\left(\xi_i P_{m_{i,1}} - \Gamma_{i,1}^{-1}\dot{\hat{\boldsymbol{\theta}}}_{i,1}\right) \\
& + \sum_{i=1}^{N}\sum_{j=2}^{n_i}\tilde{\boldsymbol{\theta}}_{i,j}^{\mathrm{T}}\left(z_{i,j}P_{m_{i,j}} - \Gamma_{i,j}^{-1}\dot{\hat{\boldsymbol{\theta}}}_{i,j}\right)
\end{aligned}
\tag{47}
$$

Substituting (45) into (47), the following inequality can be obtained

$$
\begin{aligned}
\dot{V} \le & -\sum_{i=1}^{N}\gamma_{i,1}\xi_i^2 - \sum_{i=1}^{N}\sum_{j=2}^{n_i}\gamma_{i,j}z_{i,j}^2 - \sum_{i=1}^{N}\omega_i\left(\xi_i^2\right)\xi_i^2 + \frac{1}{2}b_i^2 \\
& + \frac{1}{2}\sum_{i=1}^{N}\sum_{j=1}^{n_i}\sum_{l=1}^{N} y_l^2 \bar{h}_{i,j,l}^2(y_l) + \frac{1}{2}\sum_{i=1}^{N}\sum_{j=1}^{n_i}\varepsilon_{i,j}^2 \\
& + \sum_{i=1}^{N}\sum_{j=1}^{n_i}\eta_{i,j}\tilde{\boldsymbol{\theta}}_{i,j}^{\mathrm{T}}\hat{\boldsymbol{\theta}}_{i,j}
\end{aligned}
\tag{48}
$$

On the one hand, choosing the smooth nonnegative functions $\omega_i\left(\xi_i^2\right)$ satisfy

$$-\sum_{i=1}^{N}\omega_i\left(\xi_i^2\right)\xi_i^2+\frac{1}{2}\sum_{i=1}^{N}\sum_{j=1}^{n_i}\sum_{l=1}^{N}y_l^2\bar{h}_{i,j,l}^2(y_l)\leq 0 \tag{49}$$

On the other hand, the following inequality is easily obtained

$$\begin{aligned}\sum_{i=1}^{N}\sum_{j=1}^{n_i}\eta_{i,j}\tilde{\boldsymbol{\theta}}_{i,j}^{\mathrm{T}}\hat{\boldsymbol{\theta}}_{i,j}&\leq-\frac{1}{2}\sum_{i=1}^{N}\sum_{j=1}^{n_i}\eta_{i,j}\tilde{\boldsymbol{\theta}}_{i,j}^{\mathrm{T}}\tilde{\boldsymbol{\theta}}_{i,j}\\&+\frac{1}{2}\sum_{i=1}^{N}\sum_{j=1}^{n_i}\eta_{i,j}\boldsymbol{\theta}_{i,j}^{\mathrm{T}}\boldsymbol{\theta}_{i,j}\\&\leq-\frac{1}{2}\sum_{i=1}^{N}\sum_{j=1}^{n_i}\bar{\eta}_{i,j}\tilde{\boldsymbol{\theta}}_{i,j}^{\mathrm{T}}\Gamma_{i,j}^{-1}\tilde{\boldsymbol{\theta}}_{i,j}\\&+\frac{1}{2}\sum_{i=1}^{N}\sum_{j=1}^{n_i}\eta_{i,j}\boldsymbol{\theta}_{i,j}^{\mathrm{T}}\boldsymbol{\theta}_{i,j}\end{aligned} \tag{50}$$

where $\bar{\eta}_{i,j}=\frac{\eta_{i,j}}{\lambda_{\max}\left(\Gamma_{i,j}^{-1}\right)}$, and $\lambda_{\max}\left(\Gamma_{i,j}^{-1}\right)$ denotes the maximal eigenvalue of $\Gamma_{i,j}^{-1}$.

Combining (48) with (49) and (50), we have

$$\begin{aligned}\dot{V}\leq&-\sum_{i=1}^{N}\gamma_{i,1}\xi_i^2-\sum_{i=1}^{N}\sum_{j=2}^{n_i}\gamma_{i,j}z_{i,j}^2\\&-\frac{1}{2}\sum_{i=1}^{N}\sum_{j=1}^{n_i}\frac{\eta_{i,j}}{\lambda_{\max}\left(\Gamma_{i,j}^{-1}\right)}\tilde{\boldsymbol{\theta}}_{i,j}^{\mathrm{T}}\Gamma_{i,j}^{-1}\tilde{\boldsymbol{\theta}}_{i,j}\\&+\frac{1}{2}\sum_{i=1}^{N}\sum_{j=1}^{n_i}\varepsilon_{i,j}^2+\frac{1}{2}\sum_{i=1}^{N}\sum_{j=1}^{n_i}\eta_{i,j}\boldsymbol{\theta}_{i,j}^{\mathrm{T}}\boldsymbol{\theta}_{i,j}+\frac{1}{2}b_i^2\\\leq&-\lambda V+h\end{aligned} \tag{51}$$

where $\lambda=\min\{\lambda_1,\ldots,\lambda_N\}$, and $h=\frac{1}{2}\sum_{i=1}^{N}\sum_{j=1}^{n_i}\varepsilon_{i,j}^2+\frac{1}{2}\sum_{i=1}^{N}\sum_{j=1}^{n_i}\eta_{i,j}\boldsymbol{\theta}_{i,j}^{\mathrm{T}}\boldsymbol{\theta}_{i,j}+\frac{1}{2}b_i^2$, with $\lambda_i=\min\{4\gamma_{i,1},2\gamma_{i,j},\bar{\eta}_{i,j}:j=1,\ldots,n_i\}$, for $i=1,\ldots,N$.

Then, based on (51), we have

$$0\leq V\leq\left(V(0)-\frac{h}{\lambda}\right)e^{-\lambda t}+\frac{h}{\lambda} \tag{52}$$

According to (52) and recalling (46), it implies that all signals of the closed-loop system are bounded.

Furthermore, based on (51), the following inequality holds

$$\frac{1}{4}\sum_{i=1}^{N}\xi_i^2=\frac{1}{4}\sum_{i=1}^{N}\frac{e_i^4}{\left(\rho_i^2-e_i^2\right)^2}\leq V(0)+\frac{h}{\lambda} \tag{53}$$

Meanwhile, inequality (52) implies that the following inequality holds

$$\left(1-4\left(V(0)+\frac{h}{\lambda}\right)\right)e_i^4\leq 4\left(V(0)+\frac{h}{\lambda}\right)\left(\rho_i^4-2\rho_i^2e_i^2\right) \tag{54}$$

where $i=1,\ldots,N$.

Then, the following inequality is valid by selecting the appropriate initial conditions and design parameters

$$1-4\left(V(0)+\frac{h}{\lambda}\right)\geq 0 \tag{55}$$

Combining (54) with (55), we have

$$\rho_i^4-2\rho_i^2e_i^2\geq 0 \tag{56}$$

Inequality (56) implies that

$$|e_i|=\left|y_i-y_{d,i}\right|\leq\frac{\rho_i}{\sqrt{2}}<\rho_i \tag{57}$$

Therefore, all the tracking errors $e_i=y_i-y_{d,i}$ satisfy the predefined transient and steady-state performance. □

4 Simulation study

Example 1 In order to verify the effectiveness of the proposed control method, consider the following large-scale nonlinear system consisting of 2 subsystems

$$\begin{cases}\dot{x}_{1,1}=x_{1,2}-0.1x_{1,1}e^{0.1x_{1,1}}+y_1^3y_2\\\dot{x}_{1,2}=u_1-x_{1,1}^2x_{1,2}+\sin x_{1,2}+0.01\sin y_1\\y_1=x_{1,1}\\\dot{x}_{2,1}=x_{2,2}-0.1x_{2,1}e^{0.1x_{2,1}}+y_1y_2^4\\\dot{x}_{2,2}=u_2-x_{2,1}^2x_{2,2}+\sin x_{2,2}+0.5y_1y_2\\y_2=x_{2,1}\end{cases} \tag{58}$$

with the initial conditions are taken as $x_{1,1}(0)=0$, $x_{1,2}(0)=0$, $x_{2,1}(0)=0$ and $x_{2,2}(0)=0$. The inputs of system satisfy the following nonsymmetric saturation nonlinearity

$$u_1=\begin{cases}1, & v_1>1\\v_1, & -0.5\leq v_1\leq 1\\-0.5, & v_1<-0.5\end{cases}\quad\text{and}$$

$$u_2=\begin{cases}0.5, & v_2>0.5\\v_2, & -0.5\leq v_2\leq 0.5\\-0.5, & v_2<-0.5\end{cases}$$

In simulation, the desired trajectories $y_{d,1}$ and $y_{d,2}$ are selected as $y_{d,1}=0.5\sin(0.5t)$ and $y_{d,2}=0.4\sin(0.4t)$, respectively. The bounded prescribed performance functions are chosen as $\rho_1(t)=\rho_2(t)=(3-0.05)e^{-t}+0.05$. The controller parameters are selected as follows:

$\gamma_{1,1}=10, \gamma_{1,2}=20$, $\gamma_{2,1}=20$, $\gamma_{2,2}=5$, $\eta_{1,1}=1$, $\eta_{1,2}=1$, $\eta_{2,1}=1$, $\eta_{2,2}=1$, $\Gamma_{1,1}=\Gamma_{2,1}=0.5I_5$, $\Gamma_{1,2}=\Gamma_{2,2}=0.5I_9$, $s_1=s_2=0.1$. The simulation results are illustrated in Figs. 2, 3, 4, 5.

Figure 2 demonstrates that the satisfactory tracking control performances are obtained. Figure 3 displays that the tracking errors e_1 and e_2 satisfy the predefined transient and steady-state performance, respectively. Figure 4 shows the trajectories of u_1, v_1 and u_2, v_2, respectively. Figure 5 shows the trajectories of $x_{1,2}$ and $x_{2,2}$. It can be seen from Figs. 2, 3, 4, 5 that: (1)the system output y_i tracks the desired trajectory $y_{d,i}$, for all $i=1,2$ as well as all the closed-loop signals are bounded. (2) The tracking errors e_1 and e_2 satisfy the given predefined transient and steady-state performance $\rho_1(t)$ and $\rho_2(t)$, respectively.

Example 2 For the purpose of further clarifying the correctness and reasonableness of the proposed approach, we consider a class of actual systems consisting of triple inverted pendulums. According to [51, 52], the system model can be described as follows

$$\begin{cases} \dot{x}_{1,1}=x_{1,2} \\ \dot{x}_{1,2}=u_1+\dfrac{g}{l}\sin x_{1,1}+\dfrac{k_1a^2}{m_1l^2}(\sin y_2\cos y_2-\sin y_1\cos y_1) \\ y_1=x_{1,1} \\ \dot{x}_{2,1}=x_{2,2} \\ \dot{x}_{2,2}=u_2+\dfrac{g}{l}\sin x_{2,1}+\dfrac{k_1a^2}{m_1l^2}(\sin y_1\cos y_1-\sin y_2\cos y_2) \\ \qquad +\dfrac{k_2a^2}{m_2l^2}(\sin y_3\cos y_3-\sin y_2\cos y_2) \\ y_2=x_{2,1} \\ \dot{x}_{3,1}=x_{3,2} \\ \dot{x}_{3,2}=u_3+\dfrac{g}{l}\sin x_{3,1}+\dfrac{k_2a^2}{m_3l^2}(\sin y_2\cos y_2-\sin y_3\cos y_3) \\ y_3=x_{3,1} \end{cases} \tag{59}$$

where k_i denote the spring constants, and m_i and l denote the mass and the length of rod, respectively, for all $i=1,2,3$. g denotes gravitational acceleration and it generally taken as $g=9.8m/s^2$. a denotes the distance

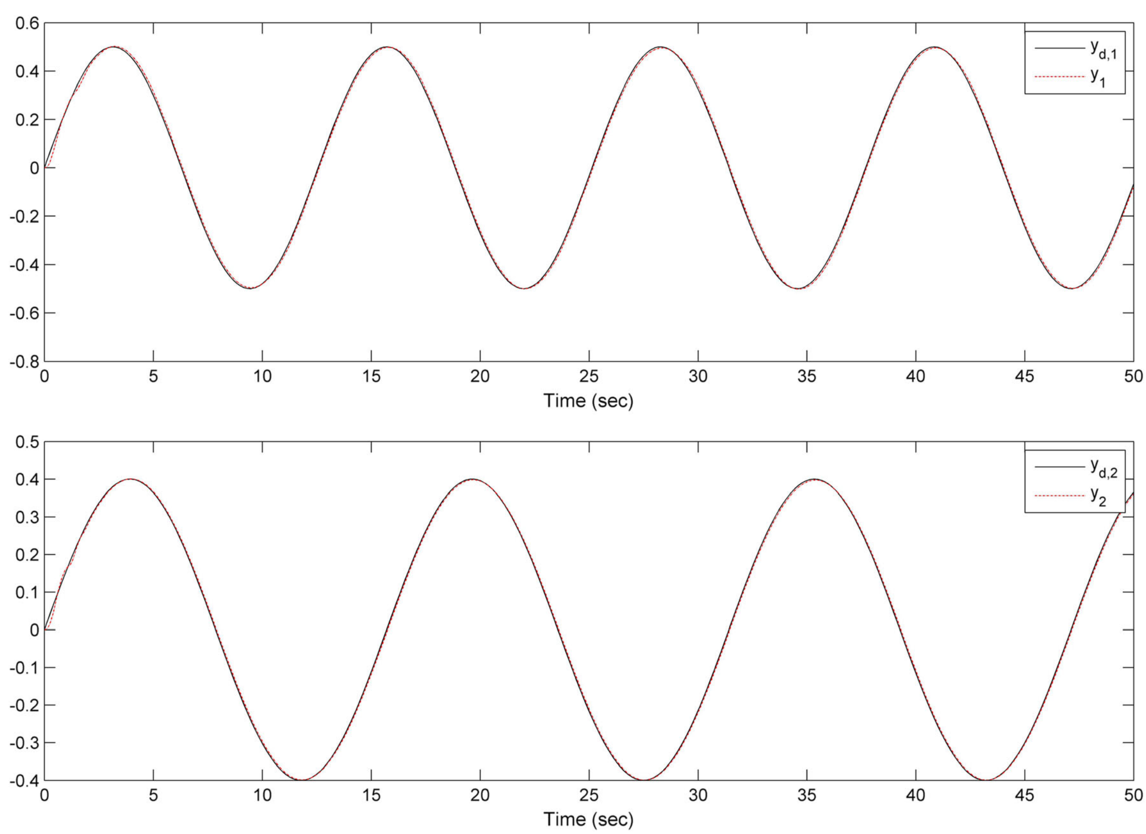

Fig. 2 The trajectories of y_1 and $y_{d,1}$, y_2 and $y_{d,2}$ of Example 1

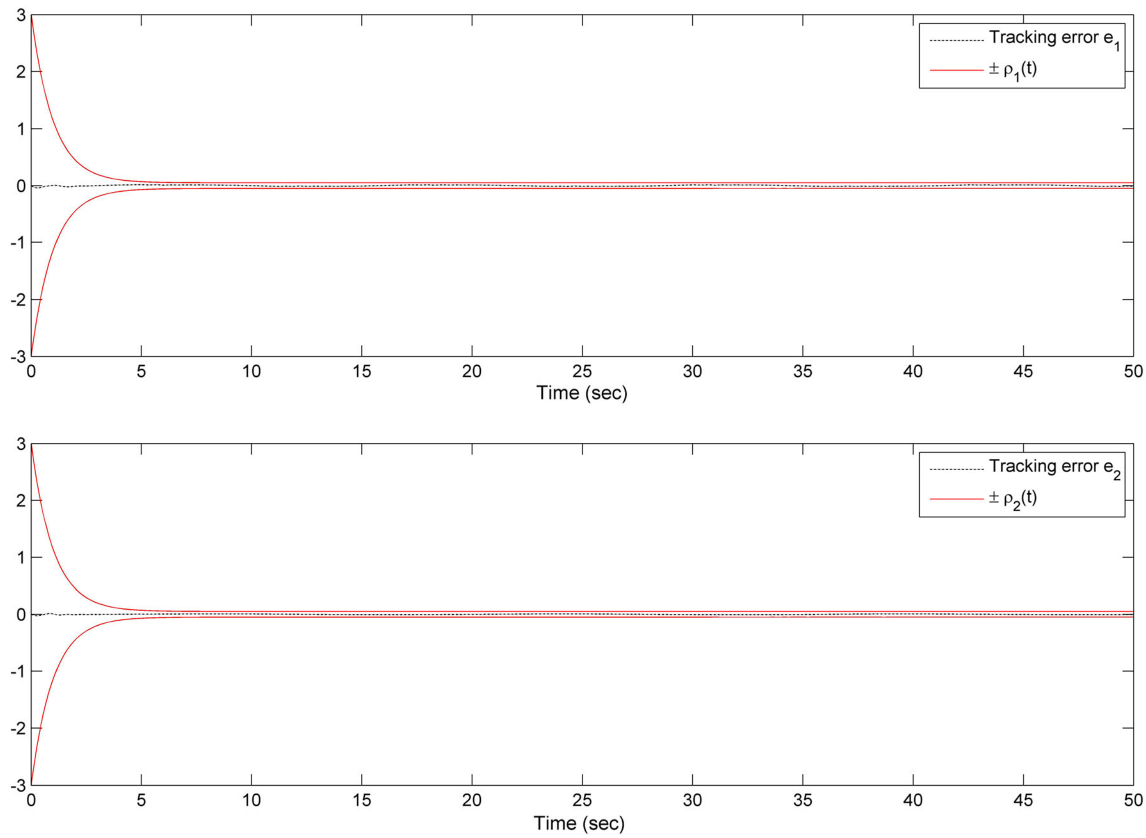

Fig. 3 The trajectories of e_1 and $\rho_1(t)$, e_2 and $\rho_2(t)$ of Example 1

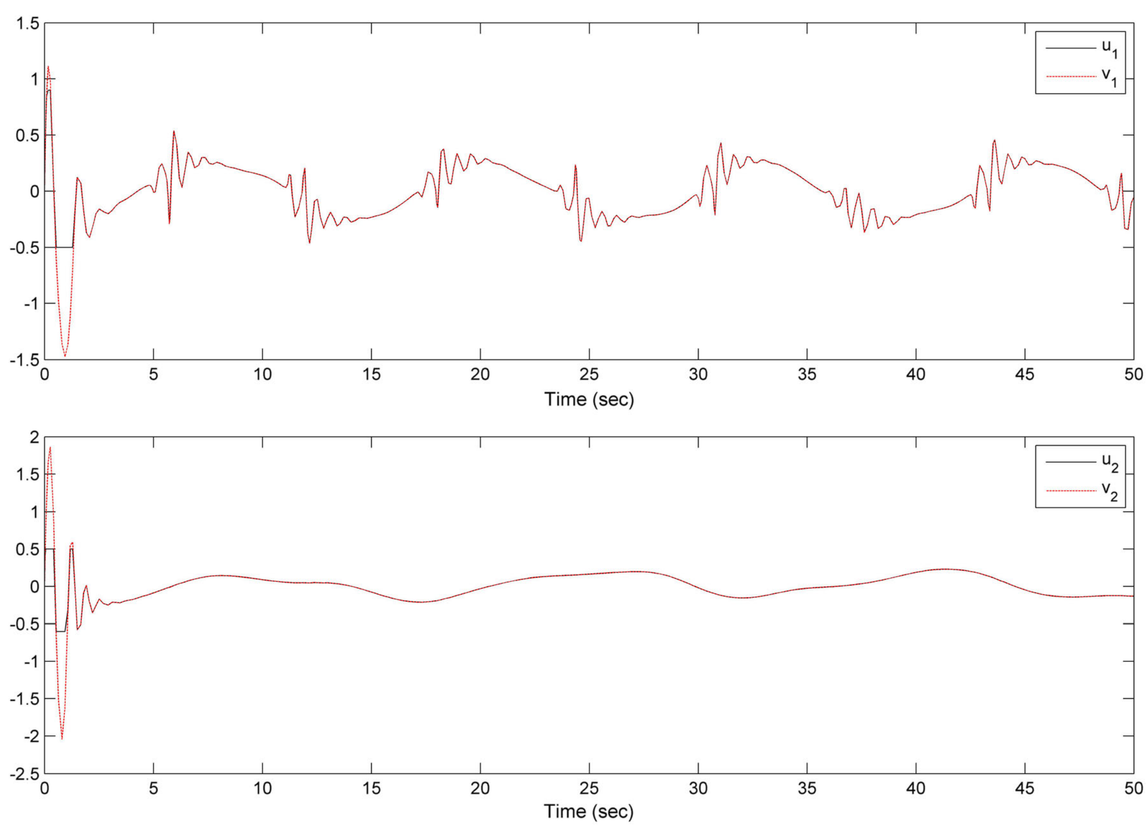

Fig. 4 The trajectories of u_1 and v_1, u_2 and v_2 of Example 1

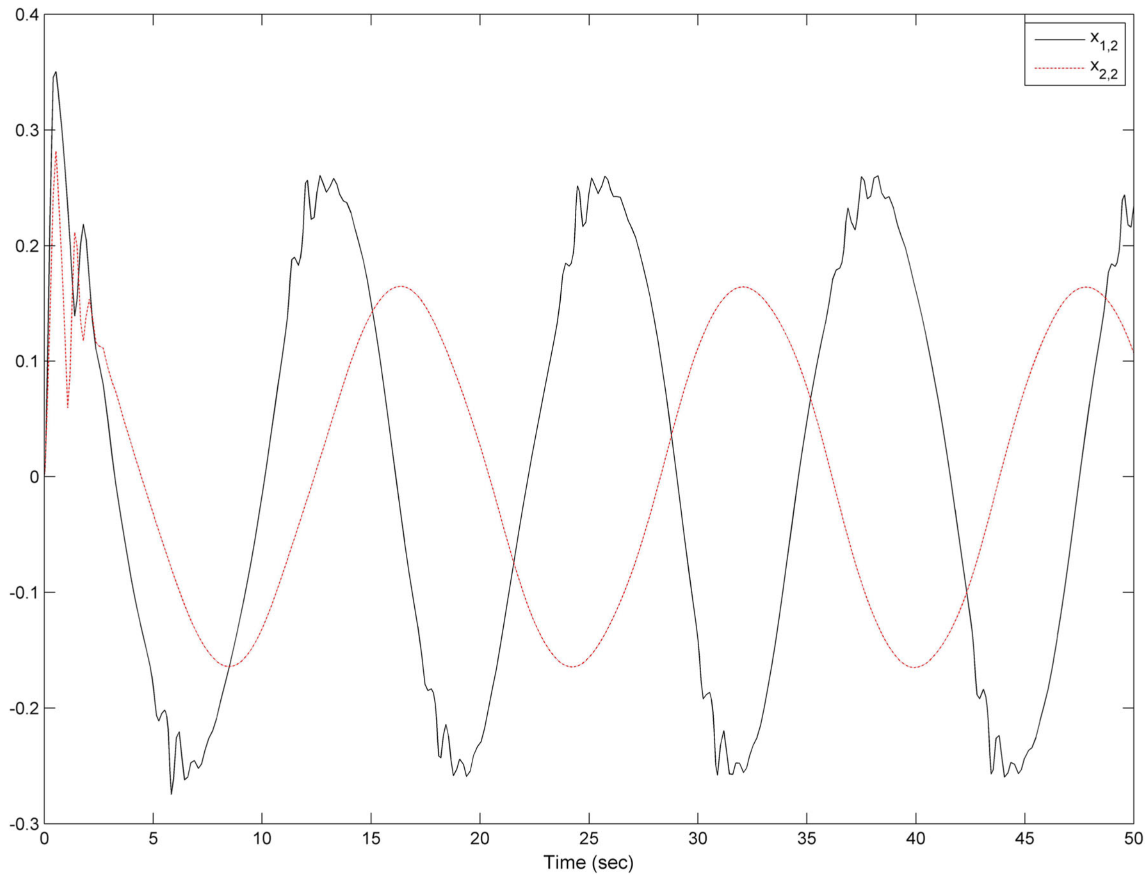

Fig. 5 The trajectories of $x_{1,2}$ and $x_{2,2}$ of Example 1

between the rod's center of and the pivot. In addition, the inputs of system satisfy the following nonsymmetric saturation nonlinearity:

$$u_1 = \begin{cases} 1, & v_1 > 1 \\ v_1, & -0.8 \le v_1 \le 1 \\ -0.8, & v_1 < -0.8 \end{cases}$$
$$u_2 = \begin{cases} 0.6, & v_2 > 0.6 \\ v_2, & -0.5 \le v_2 \le 0.6 \\ -0.5, & v_2 < -0.5 \end{cases}$$
$$u_3 = \begin{cases} 0.5, & v_3 > 0.5 \\ v_3, & -0.6 \le v_3 \le 0.5 \\ -0.6, & v_3 < -0.6 \end{cases}$$

For system (59), the desired trajectories $y_{d,1}, y_{d,2}$ and $y_{d,3}$ are selected as $y_{d,1} = 0.5\sin(0.5t)$ and $y_{d,2} = y_{d,3} = 0.4\sin(0.4t)$, respectively. The bounded prescribed performance functions are chosen as $\rho_1(t) = \rho_2(t) = \rho_3(t) = (3 - 0.05)e^{-t} + 0.05$. In simulation, on the one hand, the initial conditions of (59) are taken as $x_{1,1}(0) = x_{1,2}(0) = x_{2,1}(0) = x_{2,2}(0) = x_{3,1}(0) = x_{3,2}(0) = 0$. The parameters of (59) are selected as $k_1 = 1$, $k_2 = 1.2$, $m_1 = m_2 = m_3 = 0.5$ kg, $l = 9$ m. On the other hand, the parameters of the control structure of (59) are designed as $\gamma_{1,1} = 10$, $\gamma_{1,2} = 2$, $\gamma_{2,1} = 10$, $\gamma_{2,2} = 5$, $\gamma_{3,1} = 20$, $\gamma_{3,2} = 5$, $\eta_{1,1} = 1$, $\eta_{1,2} = 1$, $\eta_{2,1} = 1$, $\eta_{2,2} = 1$, $\eta_{3,1} = 1$, $\eta_{3,2} = 1$, $\Gamma_{1,1} = \Gamma_{2,1} = \Gamma_{3,1} = 0.5I_5$, $\Gamma_{1,2} = \Gamma_{2,2} = \Gamma_{3,2} = 0.5I_9$, $s_1 = 0.1, s_2 = 0.1, s_3 = 0.1$.

The simulation results are illustrated in Figs. 6-9. Figure 6 demonstrates that the satisfactory tracking control performances are obtained. Figure 7 displays that the tracking errors e_1, e_2 and e_3 satisfy the predefined transient and steady-state performance, respectively. Figure 8 shows the trajectories of u_1, v_1, u_2, v_2, u_3, v_3, respectively. Figure 9 shows the trajectories of $x_{1,2}$, $x_{2,2}$ and $x_{3,2}$. Obviously,

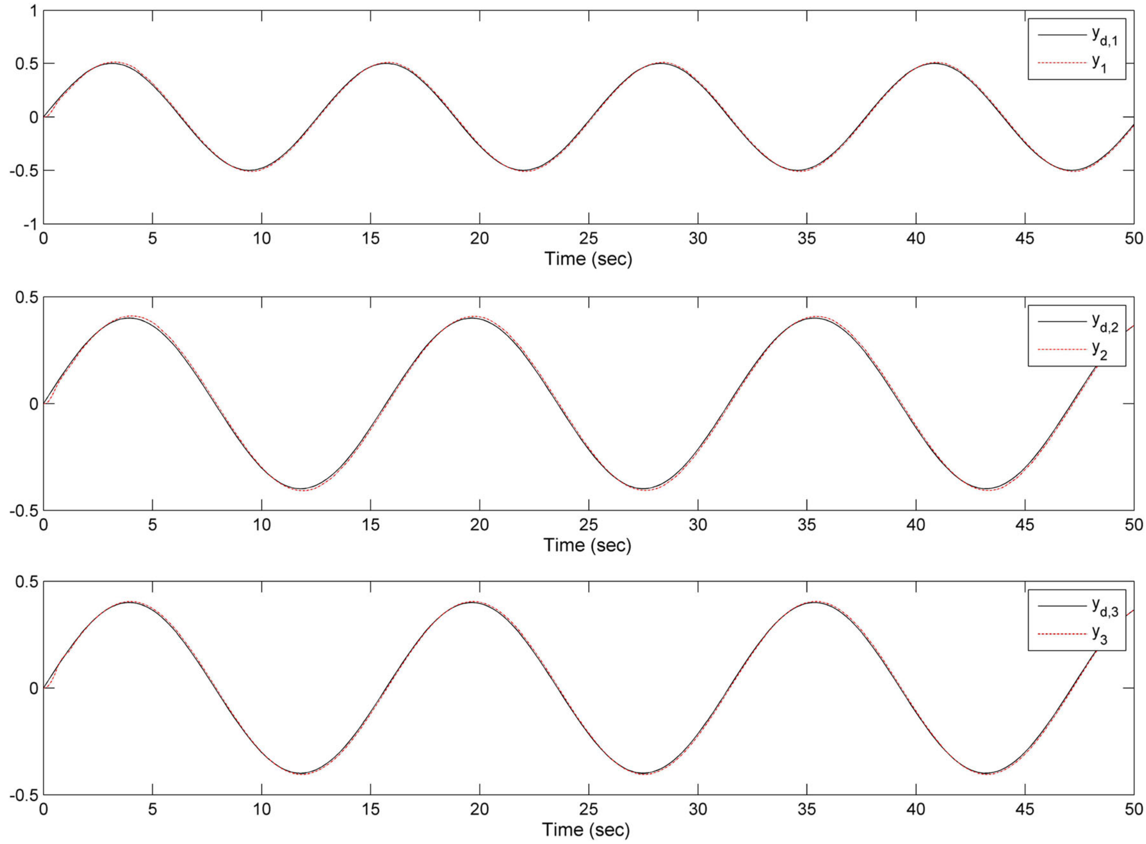

Fig. 6 The trajectories of y_1 and $y_{d,1}$, y_2 and $y_{d,2}$, y_3 and $y_{d,3}$ of Example 2

a satisfactory control effects have been obtained from Figs. 6, 7, 8, 9.

Remark 9 The result of Examples 1 and 2 show that the proposed algorithm is valid for both constructed systems and actual systems. On the one hand, it can be clearly seen that the proposed control algorithm can realize that all the signals of the given control systems are bounded, all the system outputs track the desired trajectory and all the tracking errors satisfy the predefined transient and steady-state performance, respectively. On the other hand, theoretical analysis and simulation experiments show that the proposed control algorithm can get a satisfactory control effect at the expense of low computational.

Example 3 The following experiment is employed for the sake of illustrating the validity of the proposed control method. Specifically, radial basis function (RBF) neural networks are used to replace MTNs in the control structure for the system (58). Simulation results are shown in Figs. 10 and 11.

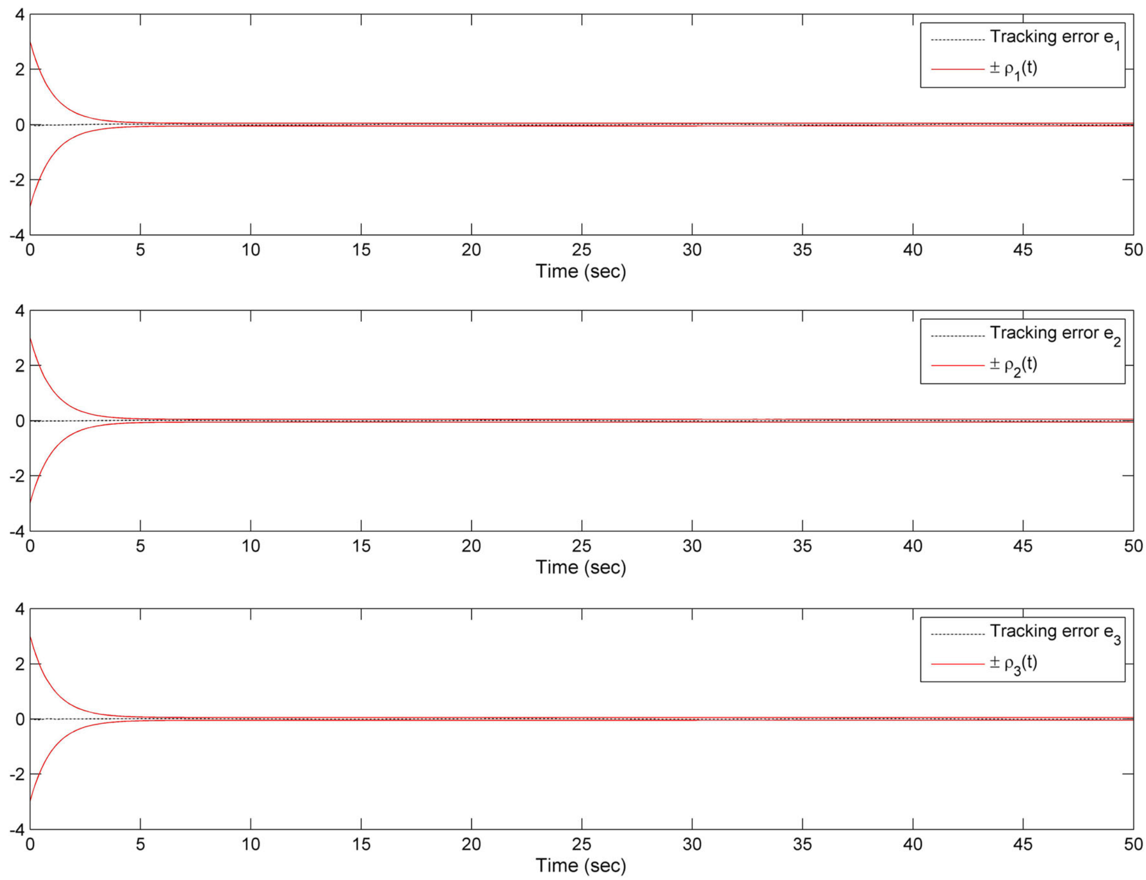

Fig. 7 The trajectories of e_1 and $\rho_1(t)$, e_2 and $\rho_2(t)$, e_3 and $\rho_3(t)$ of Example 2

According to Figs. 10 and 11, we can see that the tracking control effects of two methods are almost the same. However, compared with MTN, the structure of RBF neural network is more complicated and functions more as a calculation. Therefore, we can draw a conclusion that the proposed approach can get satisfactory results at the cost of low computational complexity.

5 Conclusion

In this study, we have developed a new adaptive decentralized MTN controller approach for the predefined performance tracking of a class of large-scale nonlinear systems subject to nonsymmetric input saturation. The proposed control approach can not only guarantee all the closed-loop signals are bounded but also all the tracking errors satisfy the predefined transient and steady-state performance. The novelty is that, for the first time, the MTN-based adaptive decentralized tracking control approach is generalised to a class of large-scale nonlinear systems, and the input saturations and the prescribed performance control are simultaneously considered.

In recent years, a growing attention has been implemented to the nonlinear systems subject to full-state constraints in view of the fact that neglecting the existence of constraints may reduce the performance of control systems. Therefore, our future research will be focused on generalizing the method proposed in this paper to the issue of full state constraints of large-scale nonlinear systems.

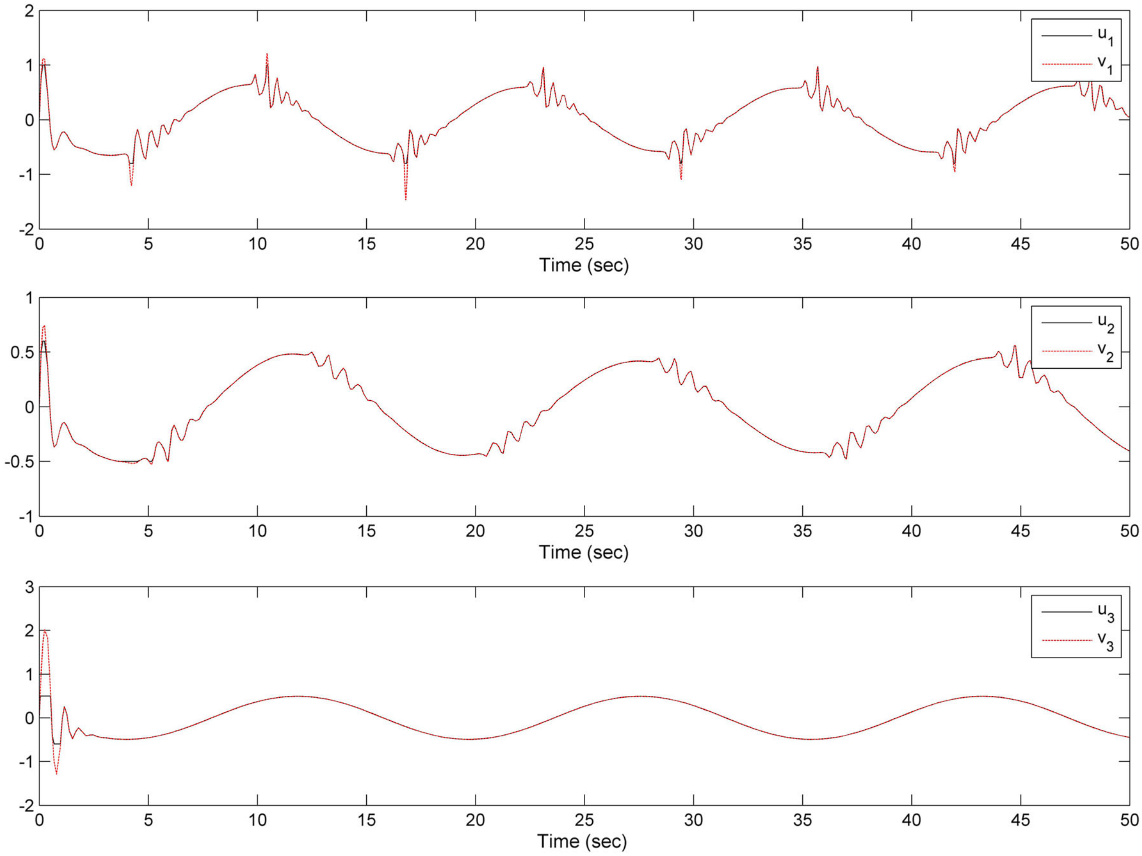

Fig. 8 The trajectories of u_1 and v_1, u_2 and v_2, u_3 and v_3 of Example 2

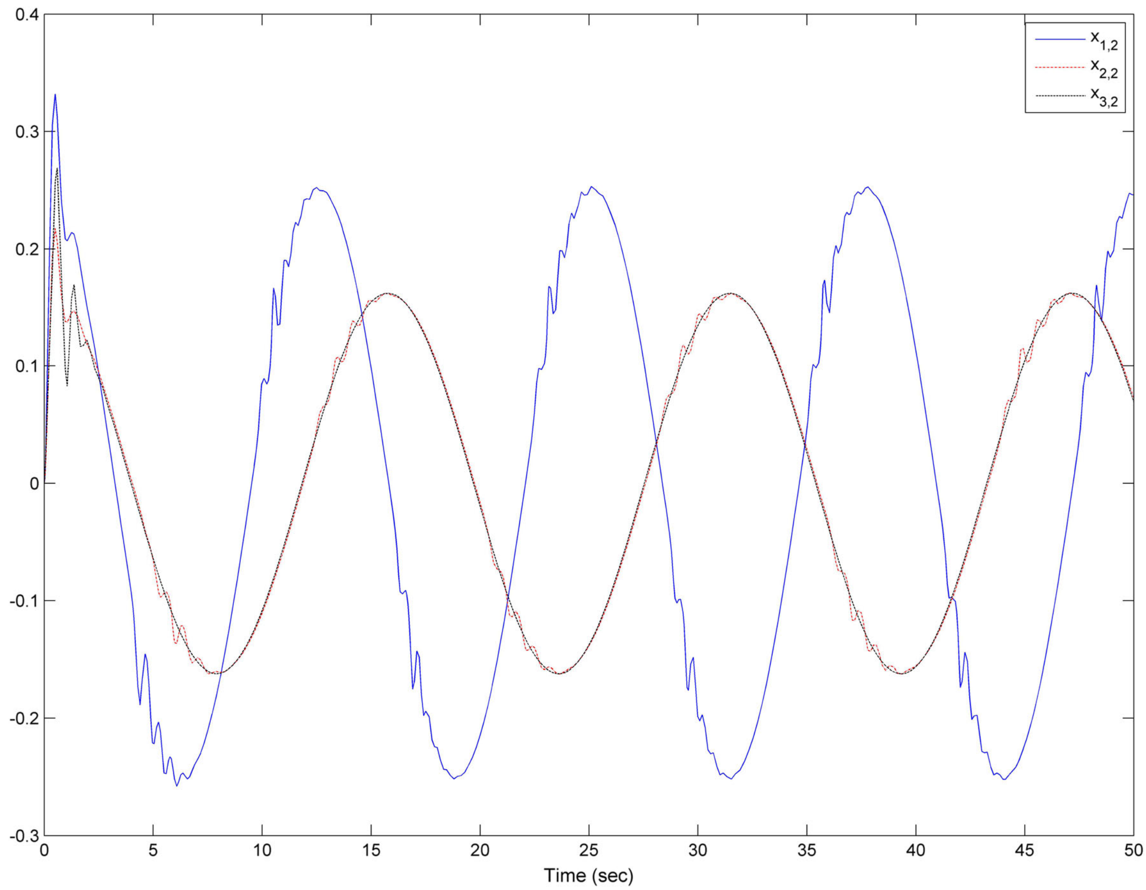

Fig. 9 The trajectories of $x_{1,2}$, $x_{2,2}$ and $x_{3,2}$ of Example 2

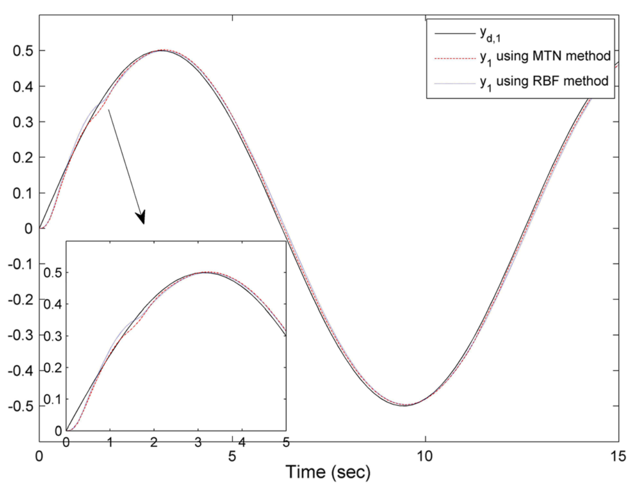

Fig. 10 The trajectories of y_1 and $y_{d,1}$ under two methods of system (58)

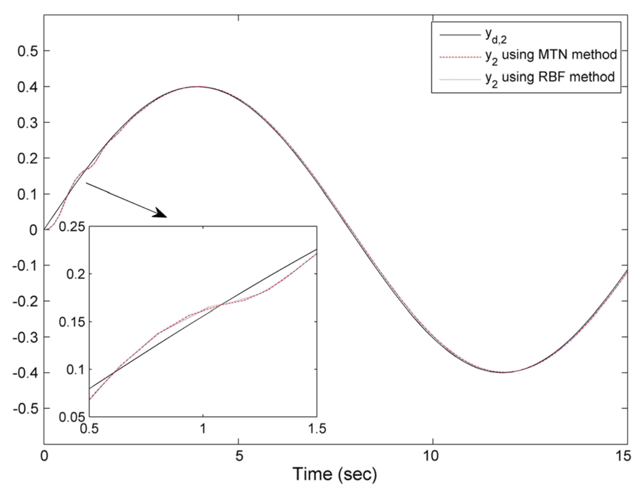

Fig. 11 The trajectories of y_2 and $y_{d,2}$ under two methods of system (58)

Funding This work was supported by the Shandong Provincial Natural Science Foundation, China (No. ZR2020QF055).

Data availability Data sharing is not applicable to this article as no datasets were generated or analysed during the current study.

Declarations

Conflict of interest The author(s) declare that they have no conflict of interest.

References

1. Mahmoud MS (2009) Decentralized stabilization of interconnected systems with time-varying delays. IEEE Trans Autom Control 54(11):2663–2668
2. Mahmoud MS, Almutairi NB (2009) Decentralized stabilization of interconnected systems with time-varying delays. Eur J Control 15(6):624–633
3. Guo Y, Jiang ZP, Hill DJ (1999) Decentralized robust disturbance attenuation for a class of large-scale nonlinear systems. Syst Control Lett 37(2):71–85
4. Jiang ZP, Repperger DW, Hill DJ (2001) Decentralized nonlinear output-feedback stabilization with disturbance attenuation. IEEE Trans Autom Control 10(46):1623–1629
5. Liu TF, Jiang ZP, Hill DJ (2012) Decentralized output-feedback control of large-scale nonlinear systems with sensor noise. Automatica 48(10):2560–2568
6. Zhang X, Liu Y (2014) Nonlinear decentralized control of large-scale systems with strong interconnections. Automatica 50(9):2419–2423
7. Liu YJ, Chen CL, Wen GX, Tong S (2011) Adaptive neural output feedback tracking control for a class of uncertain discrete-time nonlinear systems. IEEE Trans Neural Netw 22(7):1162–7
8. Han YQ, Zhu SL, Yang SG, Chu L (2021) Adaptive multi-dimensional Taylor network tracking control for a class of nonlinear systems. Int J Control 94(2):277–285
9. Wang HQ, Shi P, Li HY, Zhou Q (2017) Adaptive neural tracking control for a class of nonlinear systems with dynamic uncertainties. IEEE Trans Cybern 47(10):3075–3087
10. Wang HQ, Chen B, Lin C (2014) Adaptive neural tracking control for a class of stochastic nonlinear systems. Int J Robust Nonlinear Control 24(7):1262–1280
11. Zhu QD, Liu YC, Wen GX (2020) Adaptive neural network control for time-varying state constrained nonlinear stochastic systems with input saturation. Inf Sci 527:191–209
12. Wang HQ, Liu K, Liu XP, Chen B, Lin C (2015) Neural-based adaptive output-feedback control for a class of nonstrict-feedback stochastic nonlinear systems. IEEE Trans Cybern 45(9):1977–1987
13. Zhou Q, Shi P, Liu HH, Xu SY (2012) Neural-network-based decentralized adaptive output-feedback control for large-scale stochastic nonlinear systems. IEEE Trans Syst Man Cybern B Cybern 42(6):1608–1619
14. Han Y, Yan H (2020) Observer-based multi-dimensional Taylor network decentralised adaptive tracking control of large-scale stochastic nonlinear systems. Int J Control 93(7):1605–1618
15. Han YQ, Yan HS (2018) Adaptive multi-dimensional Taylor network tracking control for SISO uncertain stochastic non-linear systems. IET Control Theory Appl 12(8):1107–1115
16. Niu B, Wang D, Li H, Xie XJ, Alotaibi ND, Alsaadi FE (2019) A novel neural-network-based adaptive control scheme for output-constrained stochastic switched nonlinear systems. IEEE Trans Syst Man Cybern Syst 49(2):418–432
17. Niu B, Ahn CK, Li H, Liu M (2018) Adaptive control for stochastic switched nonlower triangular nonlinear systems and its application to a one-link manipulator. IEEE Trans Syst Man Cybern Syst 48(10):1701–1714
18. Tong SC, Li YM (2013) Adaptive fuzzy output feedback control of MIMO nonlinear systems with unknown dead-zone inputs. IEEE Trans Fuzzy Syst 21(1):134–146
19. Deng C, Yang GH (2017) Decentralized fault-tolerant control for a class of nonlinear large-scale systems with actuator faults. Inf Sci 382–383:334–349
20. Sun KK, Sui S, Tong SC (2018) Fuzzy adaptive decentralized optimal control for strict feedback nonlinear large-scale systems. IEEE Trans Cybern 48(4):1326–1339
21. Long LJ, Zhao J (2015) Decentralized adaptive fuzzy output-feedback control of switched large-scale nonlinear systems. IEEE Trans Fuzzy Syst 23(5):1844–1860
22. Si WJ, Dong XD, Yang FF (2018) Decentralized adaptive neural control for high-order interconnected stochastic nonlinear time-delay systems with unknown system dynamics. Neural Netw 99:123–133
23. Wang HQ, Liu PX, Bao JL, Xie XJ, Li S (2020) Adaptive neural output-feedback decentralized control for large-scale nonlinear systems with stochastic disturbances. IEEE Trans Neural Netw Learn Syst 31(3):972–983
24. Cao L, Li HY, Wang N, Zhou Q (2019) Observer-based event-triggered adaptive decentralized fuzzy control for nonlinear large-scale systems. IEEE Trans Fuzzy Syst 27(6):1201–1214
25. Esfandiari K, Abdollahi F, Talebi HA (2015) Adaptive control of uncertain nonaffine nonlinear systems with input saturation using neural networks. IEEE Trans Neural Netw Learn Syst 26(10):2311–2322
26. Song ZB, Li P, Wang Z, Huang X, Liu WH (2020) Adaptive tracking control for switched uncertain nonlinear systems with input saturation and unmodeled dynamics. IEEE Trans Circuits Syst II Express Briefs 67(12):3152–3156
27. Li HY, Bai L, Zhou Q, Lu RQ, Wang LJ (2017) Adaptive fuzzy control of stochastic nonstrict-feedback nonlinear systems with input saturation. IEEE Trans Syst Man Cybern Syst 47(8):2185–2197
28. Wang HQ, Chen B, Liu XP, Liu KF, Lin C (2014) Adaptive neural tracking control for stochastic nonlinear strict-feedback systems with unknown input saturation. Inf Sci 269:300–315
29. Zhou Q, Shi P, Tian Y, Wang MY (2015) Approximation-based adaptive tracking control for MIMO nonlinear systems with input saturation. IEEE Trans Cybern 45(10):2119–2128
30. Chen M, Zhou YL, Guo WW (2014) Robust tracking control for uncertain MIMO nonlinear systems with input saturation using RWNNDO. Neurocomputing 144:436–447
31. Wang BH, Chen WS, Zhang B (2019) Semi-global robust tracking consensus for multi-agent uncertain systems with input saturation via metamorphic low-gain feedback. Automatica 103:363–373
32. Liu XP, Wang HQ, Gao C, Chen M (2017) Adaptive fuzzy funnel control for a class of strict feedback nonlinear systems. Neurocomputing 241:71–80
33. Liu L, Wang ZS, Huang ZJ, Zhang HG (2017) Adaptive predefined performance control for MIMO systems with unknown direction via generalized fuzzy hyperbolic model. IEEE Trans Fuzzy Syst 25(3):527–542
34. Yang Y, Tan J, Yue D (2020) Prescribed performance tracking control of a class of uncertain pure-feedback nonlinear systems with input saturation. IEEE Trans Syst Man Cybern Syst 50(5):1733–1745

35. Sui S, Tong S, Li Y (2015) Observer-based fuzzy adaptive prescribed performance tracking control for nonlinear stochastic systems with input saturation. Neurocomputing 158:100–108
36. Han YQ, Li N, He WJ, Zhu SL (2021) Adaptive multi-dimensional Taylor network funnel control of a class of nonlinear systems with asymmetric input saturation. Int J Adapt Control Signal Process. https://doi.org/10.1002/acs.3224
37. Gao YF, Sun XM, Wen CY, Wang W (2017) Adaptive tracking control for a class of stochastic uncertain nonlinear systems with input saturation. IEEE Trans Autom Control 62(5):2498–2504
38. Han YQ (2020) Adaptive tracking control for a class of stochastic non-linear systems with input saturation constraint using multi-dimensional Taylor network. IET Control Theory Appl 14(9):1193–1199
39. Duan DY, Chu L, Han YQ (2020) Multi-dimensional Taylor network-based adaptive funnel tracking control of a class of nonlinear systems with prescribed performance. IEEE Access 8:132265–132272
40. Wang HQ, Zou YC, Liu PX, Liu XP (2018) Robust fuzzy adaptive funnel control of nonlinear systems with dynamic uncertainties. Neurocomputing 314:299–309
41. Li S, Guo J, Xiang ZR (2018) Sampled-data adaptive prescribed performance control of a class of nonlinear systems. Neurocomputing 283:282–292
42. Bu XW, He GJ, Wei DZ (2018) A new prescribed performance control approach for uncertain nonlinear dynamic systems via back-stepping. J Franklin Inst 355(17):8510–8536
43. Wang CC, Yang GH (2018) Observer-based adaptive prescribed performance tracking control for nonlinear systems with unknown control direction and input saturation. Neurocomputing 284:17–26
44. Liu CG, Liu XP, Wang HQ, Zhou YC, Lu SY, Xu B (2020) Event-triggered adaptive tracking control for uncertain nonlinear systems based on a new funnel function. ISA Trans 99:130–138
45. Ouyang XY, Wu LB, Zhao N, Gao C (2020) Event-triggered adaptive prescribed performance control for a class of pure-feedback stochastic nonlinear systems with input saturation constraints. Int J Syst Sci 51(12):2238–2257
46. Cheng C, Zhang Y, Liu SY (2019) Neural observer-based adaptive prescribed performance control for uncertain nonlinear systems with input saturation. Neurocomputing 370:94–103
47. Wang HQ, Chen B, Liu XP, Liu KF, Lin C (2013) Robust adaptive fuzzy tracking control for pure-feedback stochastic nonlinear systems with input constraints. IEEE Trans Cybern 43(6):2093–2104
48. Han YQ (2020) Adaptive tracking control for a class of stochastic non-linear systems with input delay: a novel approach based on multi-dimensional Taylor network. IET Control Theory Appl 14(15):2147–2153
49. Li J, Chen WS, Li JM (2011) Adaptive NN output-feedback decentralized stabilization for a class of large-scale stochastic nonlinear strict-feedback systems. Int J Robust Nonlinear Control 21(4):452–472
50. Chen B, Liu X, Liu K, Lin C (2009) Novel adaptive neural control design for nonlinear MIMO time-delay systems. Automatica 45(6):1554–1560
51. Du PH, Pan YN, Li HY, Lam HK (2020) Nonsingular finite-time event-triggered fuzzy control for large-scale nonlinear systems. IEEE Trans Fuzzy Syst. https://doi.org/10.1109/TFUZZ.2020.2992632
52. Yoo SJ, Park JB, Choi YH (2009) Decentralized adaptive stabilization of interconnected nonlinear systems with unknown non-symmetric dead-zone inputs. Automatica 45(2):436–443
53. Mohammadzadeh A, Hashemzadeh F (2015) A new robust observer-based adaptive type-2 fuzzy control for a class of non-linear systems. Appl Soft Comput 37:204–216
54. Balootaki MA, Rahmani H, Moeinkhah H, Mohammadzadeh A (2020) On the synchronization and stabilization of fractional-order chaotic systems: recent advances and future perspectives. Phys A Stat Mech Appl 551:124203
55. Mohammadzadeh A, Kumbasar T (2020) A new fractional-order general type-2 fuzzy predictive control system and its application for glucose level regulation. Appl Soft Comput 91:106241
56. Mosavi A, Qasem SN, Shokri M, Band SS, Mohammadzadeh A (2020) Fractional-order fuzzy control approach for photovoltaic/battery systems under unknown dynamics, variable irradiation and temperature. Electronics 9(9):1455
57. Mohammadzadeh A, Kaynak O (2020) A novel fractional-order fuzzy control method based on immersion and invariance approach. Appl Soft Comput 88:106043